The Journal of Chemical Physics

On the geometric dependence of the molecular dipole polarizability in water: A benchmark study of higher-order electron correlation, basis set incompleteness error, core electron effects, and zero-point vibrational contributions

Cite as: J. Chem. Phys. **149**, 204303 (2018); https://doi.org/10.1063/1.5051458
Submitted: 08 August 2018 . Accepted: 11 October 2018 . Published Online: 26 November 2018

Ka Un Lao, Junteng Jia, Rahul Maitra, and Robert A. DiStasio

COLLECTIONS

This paper was selected as Featured

View Online Export Citation CrossMark

ARTICLES YOU MAY BE INTERESTED IN

Perspective: Computational chemistry software and its advancement as illustrated through three grand challenge cases for molecular science
The Journal of Chemical Physics **149**, 180901 (2018); https://doi.org/10.1063/1.5052551

A consistent and accurate ab initio parametrization of density functional dispersion correction (DFT-D) for the 94 elements H-Pu
The Journal of Chemical Physics **132**, 154104 (2010); https://doi.org/10.1063/1.3382344

Understanding non-covalent interactions in larger molecular complexes from first principles
The Journal of Chemical Physics **150**, 010901 (2019); https://doi.org/10.1063/1.5075487

Lock-in Amplifiers up to 600 MHz
starting at
$6,210

Zurich Instruments
Watch the Video

© 2018 Author(s).

THE JOURNAL OF CHEMICAL PHYSICS **149**, 204303 (2018)

On the geometric dependence of the molecular dipole polarizability in water: A benchmark study of higher-order electron correlation, basis set incompleteness error, core electron effects, and zero-point vibrational contributions

Ka Un Lao, Junteng Jia, Rahul Maitra, and Robert A. DiStasio, Jr.[a)]
Department of Chemistry and Chemical Biology, Cornell University, Ithaca, New York 14853, USA

(Received 8 August 2018; accepted 11 October 2018; published online 26 November 2018)

In this work, we investigate how geometric changes influence the static dipole polarizability (α) of a water molecule by explicitly computing the corresponding dipole polarizability surface (DPS) across 3125 total (1625 symmetry-unique) geometries using linear response coupled cluster theory including single, double, and triple excitations (LR-CCSDT) and the doubly augmented triple-ζ basis set (d-aug-cc-pVTZ). Analytical formulae based on power series expansions of this *ab initio* surface are generated using linear least-squares analysis and provide highly accurate estimates of this quantity as a function of molecular geometry (i.e., bond and angle variations) in a computationally tractable manner. An additional database, which consists of 25 representative molecular geometries and incorporates a more thorough treatment of both basis sets and core electron effects, is provided as a current benchmark for this quantity and the corresponding leading-order C_6 dispersion coefficient. This database has been utilized to assess the importance of these effects as well as the relative accuracy that can be obtained using several quantum chemical methods and a library of density functional approximations. In addition to high-level electron correlation methods (like CCSD) and our analytical least-squares formulae, we find that the SCAN0, PBE0, MN15, and B97-2 hybrid functionals yield the most accurate descriptions of the molecular polarizability tensor in H_2O. Using first-order perturbation theory, we compute the zero-point vibrational correction to α at the CCSDT/d-aug-cc-pVTZ level and find that this correction contributes approximately 3% to the isotropic (α_{iso}) and nearly 50% to the anisotropic (α_{aniso}) polarizability values. In doing so, we find that α_{iso} = 9.8307 bohr^3, which is in excellent agreement with the experimental value of 9.83 ± 0.02 bohr^3 provided by Russell and Spackman. The DPS reported herein provides a benchmark-quality quantum mechanical estimate of this fundamental quantity of interest and should find extensive use in the development (and assessment) of next-generation force fields and machine-learning based approaches for modeling water in complex condensed-phase environments. *Published by AIP Publishing.* https://doi.org/10.1063/1.5051458

I. INTRODUCTION

The dipole polarizability describes the changes in the charge distribution of an atom or a molecule that are induced by the presence of an external electric field. As such, this molecular response property is a central ingredient in many important phenomena, including the Stark effect, dielectric polarization, and intermolecular forces (such as induction and dispersion).[1–4] The molecular polarizability of water, in particular, is still of significant interest today, as demonstrated by a number of recent experimental and theoretical efforts, such as spectroscopic studies,[5] molecular simulations,[6] and intermolecular potential (force field) developments,[7–10] to name a few. However, high-accuracy benchmark *ab initio* calculations of this fundamental response property can be very challenging and often require a sophisticated treatment of electron correlation in conjunction with quite diffuse basis sets to obtain sufficiently converged results.[11]

Various aspects concerning the theoretical determination of the electronic contribution to the dipole polarizability have been examined for the water molecule (in particular, at its equilibrium geometry) over the past four decades and include quantum mechanical treatments at the level of second-order Møller-Plesset perturbation theory (MP2),[11–25] fourth-order Møller-Plesset perturbation theory (MP4),[14,26] multi-configurational self-consistent field theory (MCSCF),[17,27–30] coupled cluster (CC) theory,[11,14,17,18,23,24,30–44] W4 theory,[45] and a comprehensive range of density functionals.[11,19,20,24–26,38,42,43,46–52] Quite often, the vibrational contributions to this property, which are due to a distortion of the molecular vibrational motion by the electric field, are neglected in purely theoretical calculations. However, vibrational polarizabilities that have been indirectly determined from experimental IR-active band intensities have indicated that these contributions are non-negligible[53] and have been estimated to contribute approximately 3% to the total (electronic + vibrational) polarizability of water.[37,54] Although much work has been devoted to estimate the vibrational contributions[55,56] to the molecular

[a)]Email: distasio@cornell.edu

polarizability of water, such as Hartree-Fock (HF),[16,28,54,57–59] complete active space self-consistent field theory (CASSCF),[27–29] MP2,[16,54,60] density functional theory (DFT),[26,51] vibrational structure theory,[39] coupled cluster singles and doubles (CCSD) with the W6 basis set (and Gauss-Hermite numerical quadrature over the lowest vibrational state),[37] and DFT-based Born–Oppenheimer molecular dynamics (BOMD),[41] theoretical approaches that accurately account for both electron correlation effects and basis set incompleteness error in this quantity are also rather scarce.

Accurate knowledge of the molecular polarizability of water is critical for the development of polarizable force fields based on non-rigid (flexible) water molecules.[7,61–64] In this case, a quantitative measure of the dependence of the polarizability on the underlying geometry is an essential first step towards describing intermolecular interactions in complex aqueous environments.[37,44,65,66] To address this need, Avila[37] computed the static dipole polarizability of water at 521 different geometries using linear response coupled cluster theory (in particular, LR-CCSD) and the W6 basis set, with further refinements using orbital-relaxed finite-field CCSD(T) for an additional subset of 20 geometries. Based on these calculations, Avila pointed out that polarizabilities computed with LR-CCSD (a method which is equivalent to orbital-unrelaxed finite-field CCSD,[67,68] in which the electric field perturbation is switched on during the solution of the CC equations only) agreed to within 1% of the orbital-relaxed finite-field CCSD(T) results.[37] Loboda *et al.*[44] then studied the geometric dependence of the static dipole polarizability (as well as mixed and higher-order polarizabilities) of water at 125 different geometries using orbital-relaxed finite-field CCSD(T) and the aug-cc-pVTZ basis set. In a detailed study which focused on the equilibrium geometry, Hammond *et al.*[11] demonstrated that while electron correlation effects beyond CCSD are non-negligible (i.e., with the triples contributing ≈1%), basis set incompleteness error plays an even more critical role in the convergence of this property. In this regard, there is strong evidence that basis sets of at least triple-ζ quality which have been augmented with two sets of diffuse functions (e.g., the d-aug-cc-pVXZ basis sets of Woon and Dunning[69] with X ≥ T) are required for convergence of this response property in the water monomer, while further augmentation (e.g., as provided by the t-aug-cc-pVXZ and q-aug-cc-pVXZ basis set series) is usually not necessary.[11,36]

With this in mind, the main goal of the present study is to benchmark how geometric changes influence the static dipole polarizability of a water molecule by explicitly computing the corresponding dipole polarizability surface (DPS) using an accurate treatment of both electron correlation and basis set effects. This is accomplished using linear response coupled cluster theory including single, double, and triple excitations (LR-CCSDT) and the doubly augmented triple-ζ basis set (d-aug-cc-pVTZ) across 3125 total (1625 symmetric-unique) molecular geometries. By simultaneously accounting for both electron correlation effects (beyond the CCSD level) and basis set incompleteness error across the most comprehensive number of non-equilibrium water geometries considered to date, this surface should find extensive use in the development (and assessment) of next-generation force fields[70] and machine-learning based approaches for computing tensorial properties.[71,72]

The remainder of the paper is organized as follows. In Sec. II, we describe the computational approach utilized throughout this work. In Sec. III, we provide a detailed analysis of the geometric dependence underlying the DPS for water as well as analytical formulae for generating these quantities obtained via linear least-squares analysis. We expect that such geometry-dependent formulae [in conjunction with the best available potential energy surfaces (PESs) and dipole moment surfaces for the water molecule][73–75] should be useful for developing new aqueous force fields and/or refining current *ab initio* based water models such as TTM,[76–79] CC-pol,[80] WHBB,[81] and MB-pol.[70] An additional database consisting of 25 representative geometries that incorporates a more thorough treatment of both basis set and core electron effects is also provided as a current benchmark for this quantity and the corresponding C_6 dispersion coefficients. This database is then utilized to assess the importance of these effects as well as the relative accuracy associated with a number of popular quantum chemical and density functional approximations. By including zero-point (ZP) vibrational contributions (which have been calculated herein for the first time at the CCSDT/d-aug-cc-pVTZ level of theory) to our highly accurate electronic polarizabilities, the currently debatable experimental results for the static polarizability of the water molecule[54,82–87] should be largely settled by comparison with our nearly exact quantum mechanical results. Final conclusions are then drawn in Sec. IV.

II. COMPUTATIONAL DETAILS

A. Construction and least-squares fits of the DPS-H_2O-3K database

The geometric dependence of the dipole polarizability (α) for an isolated (gas-phase) water molecule is obtained by fitting the corresponding DPS (centered around the experimental equilibrium geometry) to a power series expansion formula. In this work, the experimental equilibrium geometry of the water molecule was taken from Ref. 88, with vibrationally averaged values of r_0 = 0.9578 Å for the OH bond length and θ_0 = 104.4776° for the HOH angle. Throughout this work, the subscript "0" in r_0 and θ_0 indicates that these are vibrationally averaged quantities obtained from experiment. The subscript "e" will be used below to denote quantities that correspond to the (global) minimum of a potential energy surface (PES) computed at a specific level of theory. A local reference frame was chosen such that each water molecule is located on the xz plane with the z-axis bisecting the HOH angle (see Fig. 1). This choice for the molecular orientation yields a sparse polarizability tensor in which the $\alpha_{xy} = \alpha_{yx}$ and $\alpha_{yz} = \alpha_{zy}$ components are strictly zero. To construct the DPS, the HOH angle (θ) was sampled at five different values (75°, 90°, θ_0 = 104.4776°, 120°, and 135°) and the OH bond lengths (r_1 and r_2) were varied between 0.650 Å and 1.298 Å in increments of 0.027 Å. This results in a total of 3125 non-equilibrium geometries that will be utilized to generate the DPS database, which we denote by DPS-H_2O-3K.

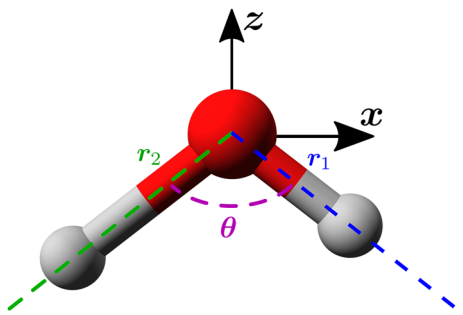

FIG. 1. The local reference frame chosen for the water molecule has all atoms located on the xz plane and the z-axis bisecting the HOH angle (θ). Throughout this work, the OH bond lengths (r_1 and r_2) in the symmetry-unique geometries are taken such that $r_1 \leq r_2$.

Due to symmetry considerations, only 1625 symmetry-unique geometries (for which $r_1 \leq r_2$) were required, which included 1500 geometries with C_s symmetry and 125 geometries with C_{2v} symmetry. To simultaneously account for both electron correlation and basis set effects, the molecular α for this set of geometries were computed at the LR-CCSDT/d-aug-cc-pVTZ level of theory, i.e.,

$$\alpha_{uv} = \alpha_{uv}^{\text{LR-CCSDT/daTZ}}, \tag{1}$$

wherein we have used u and v to denote Cartesian axes and daXZ to denote the d-aug-cc-pVXZ (with X = D, T, Q, 5) basis set. Tabulated data for the DPS-H_2O-3K database [as well as the corresponding energies (V) and dipole moments (μ)] computed at the CCSDT/daTZ level can be found in Table S1 of the supplementary material.

The non-zero components of the molecular α tensor in the DPS-H_2O-3K database have been fitted to the following power series expansion formula:[37,44,64,89–91]

$$\begin{aligned}\alpha_{uv}^{\text{pred}} &= \sum_{i+j+k=0}^{p} \varphi_{ijk}^{(uv)} (\Delta h_1)^i (\Delta h_2)^j (\Delta h_3)^k \\ &\equiv \sum_{i+j+k=0}^{p} \varphi_{ijk}^{(uv)} f_{ijk},\end{aligned} \tag{2}$$

in which $\varphi_{ijk}^{(uv)}$ are the expansion coefficients and $\alpha_{uv}^{\text{pred}}$ is the predicted value for α_{uv}. In this expression, Δh_1, Δh_2, and Δh_3 are the normalized deviations from the experimental equilibrium geometry, which are defined as

$$\Delta h_1 = \frac{\theta - \theta_0}{\theta_0}, \quad \Delta h_2 = \frac{r_1 - r_0}{r_0}, \quad \Delta h_3 = \frac{r_2 - r_0}{r_0}. \tag{3}$$

Powers of these normalized deviations were chosen as features (f_{ijk}) during the fitting procedure in this statistical model. The power series expansion in Eq. (2) was limited to order p (i.e., $0 \leq i + j + k \leq p$), which gives rise to a total of M expansion coefficients. For all values of p, $\varphi_{000}^{(uv)}$ was acquired from the components of α at the experimental equilibrium geometry.

For each non-zero component of α, a linear least-squares procedure was used to determine the $\{\varphi_{ijk}^{(uv)}\}$ for $i + j + k \neq 0$ that minimize the following prediction error:

$$\{\varphi_{ijk}^{(uv)}\} = \arg \min_{\{\varphi_{ijk}^{(uv)}\}} \left\{ \sum_{q=1}^{N} \left[\alpha_{uv}^{\text{pred}}(q) - \alpha_{uv}(q) \right]^2 \right\}, \tag{4}$$

in which q runs over the $N = 3125$ computed α_{uv} values in the DPS-H_2O-3K database. In matrix notation, this is equivalent to

$$\beta = \arg \min_{\beta} \|\mathbf{A}\beta - y\|_2^2, \tag{5}$$

where $\mathbf{A}^{N\times(M-1)}$ is a matrix containing the features for a given water geometry in each row, $\beta^{(M-1)\times 1}$ is a vector that contains the expansion coefficients, and $y^{N\times 1}$ is a vector that contains the calculated (reference) polarizabilities. With $\mathbf{A} = \mathbf{U\Sigma V}^T$ as the exact singular value decomposition (SVD) of the $\mathbf{A}$ matrix, the solution of this linear least-squares problem is given by

$$\beta = \mathbf{V\Sigma}^{-1}\mathbf{U}^T y. \tag{6}$$

To improve the conditioning of our fitting procedure, only t singular values with $\sigma_i > 10^{-5} \times \sigma_{\max}$ (with $\sigma_{\max}$ denoting the maximum singular value) and their corresponding singular vectors were kept during the SVD procedure. The resulting approximate SVD of $\mathbf{A}$ is thus given by $\mathbf{A} \approx \mathbf{U}_t\mathbf{\Sigma}_t\mathbf{V}_t^T$, and the corresponding least-squares solution,

$$\beta = \mathbf{V}_t\mathbf{\Sigma}_t^{-1}\mathbf{U}_t^T y, \tag{7}$$

is more numerically stable with respect to small perturbations δy.

B. Construction of the benchmark DPS-H_2O-25++ and C6S-H_2O-25++ databases

To account for basis set effects (beyond the daTZ level) and core electron contributions to these quantities, we also constructed a smaller benchmark database, in which five OH bond configurations (three C_{2v} geometries with: $r_1 = r_2 = 0.650$ Å, $r_1 = r_2 = r_0 = 0.9578$ Å, and $r_1 = r_2 = 1.298$ Å; two C_s geometries with: $r_1 = 0.650$ Å and $r_2 = r_0 = 0.9578$ Å, $r_1 = r_0 = 0.9578$ Å and $r_2 = 1.298$ Å) were chosen for each of the five angles above ($\theta = 75°$, $\theta = 90°$, $\theta = \theta_0 = 104.4776°$, $\theta = 120°$, and $\theta = 135°$) for a total of $5 \times 5 = 25$ geometries. These 25 geometries were chosen to span the more extensively sampled collection of 3125 total (1625 symmetry-unique) geometries utilized to build the DPS-H_2O-3K surface described above.

Molecular α in the benchmark DPS-H_2O-25++ database were computed via the following prescription:

$$\alpha_{uv} = \alpha_{uv}^{\text{LR-CCSDT/daQZ}} + \Delta\alpha_{\text{basis}} + \Delta\alpha_{\text{core}}, \tag{8}$$

which includes a baseline calculation of α_{uv} at the LR-CCSDT/daQZ level of theory (which utilizes the larger daQZ basis set than that in the more extensive DPS-H_2O-3K database) as well as further corrections for basis set incompleteness error,

$$\Delta\alpha_{\text{basis}} = \alpha_{uv}^{\text{LR-CCSD/da5Z}} - \alpha_{uv}^{\text{LR-CCSD/daQZ}}, \tag{9}$$

and core electron contributions to α,

$$\Delta\alpha_{\text{core}} = \alpha_{uv}^{\text{LR-CCSD[FULL]/daCQZ}} - \alpha_{uv}^{\text{LR-CCSD/daQZ}}. \tag{10}$$

In this last expression, daCQZ denotes the d-aug-cc-pCVQZ basis set,[92] which provides additional functions to better describe core-valence electron correlation, and LR-CCSD[FULL] denotes that all electrons (including the core electrons) were included in the calculation. We note in passing that all other LR-CC and CC calculations (without the [FULL] designation) in this work employed the frozen core

approximation. The corresponding refined V and μ for these 25 geometries can be found in Table S2.

This benchmark database was used to critically assess the performance of the HF, MP2, and CCSD quantum chemistry (QC) methodologies, the analytical least-squares formulae, and a wide range of DFT functionals including LDA/LSDA,[93,94] the BLYP[95,96] and PBE[97] generalized-gradient approximation (GGA) functionals, the widely used B3LYP[98,99] and PBE0[100] hybrid functionals, the M11,[101] B97-2,[50] and ωB97X-D[102] functionals (which are recommended for calculating α in Refs. 25, 26, and 41, respectively), the most recent Minnesota functional MN15,[103] the recently developed non-local functionals of Mardirossian and Head-Gordon (B97M-V,[104] ωB97X-V,[105] and ωB97M-V),[106] the recently developed meta- and hyper-GGA functionals of Perdew and co-workers (MS2,[107] MS2h,[107] MVS,[108] MVSh,[108] and SCAN),[109] the SCAN0 hybrid functional proposed by Hui and Chai,[110] and the mBEEF functional, which is based on the Bayesian error estimation functional framework.[111] Orbital-relaxed α at the HF, MP2, and DFT levels were computed from first derivatives of the respective μ, obtained using the finite-field method with an applied electric field strength of $1.889\,726\,125 \times 10^{-5}$ a.u. Orbital-unrelaxed α at the MP2 level were computed via the second derivatives of the MP2 energy using the finite-field method in which the electric-field perturbation was only switched on after convergence of the HF equations. This ensures the use of field-free molecular orbitals during the calculation of the perturbative correction.

In addition to the non-zero Cartesian components of the α tensor, the spherically isotropic (α_{iso}) and anisotropic (α_{aniso}) polarizabilities were also computed using

$$\alpha_{\text{iso}} = \frac{1}{3}(\alpha_{xx} + \alpha_{yy} + \alpha_{zz}) \tag{11}$$

and

$$\alpha_{\text{aniso}} = \frac{1}{\sqrt{2}}\Big[(\alpha_{xx} - \alpha_{yy})^2 + (\alpha_{yy} - \alpha_{zz})^2 + (\alpha_{zz} - \alpha_{xx})^2 + 6(\alpha_{xy}^2 + \alpha_{xz}^2 + \alpha_{yz}^2)\Big]^{1/2}. \tag{12}$$

Leading-order isotropic dispersion coefficients ($C_{6,\text{iso}}$) for these 25 representative geometries were obtained via the Casimir-Polder integral,[112]

$$C_{6,\text{iso}} = \frac{3}{\pi}\int_0^\infty d\omega\, \alpha_{\text{iso}}(i\omega)\alpha_{\text{iso}}(i\omega), \tag{13}$$

in which $\alpha_{\text{iso}}(i\omega)$ is the frequency-dependent isotropic dipole polarizability (for imaginary frequencies). The required set of $\alpha_{\text{iso}}(i\omega)$ were obtained via the Cauchy moment expansion at the LR-CC level[113,114] with use of the $[n, n-1]_\beta$ Padé approximant, as recommended by Langhoff and Karplus.[115] With $n = 5$, the resulting C_6 dispersion coefficients are expected to be converged to within 1%.[113]

Molecular $C_{6,\text{iso}}$ dispersion coefficients in the benchmark C6S-H_2O-25++ database were computed via the following prescription:

$$C_{6,\text{iso}} = C_{6,\text{iso}}^{\text{LR-CCSD/daQZ}} + \Delta C_{6,\text{basis}} + \Delta C_{6,\text{core}}, \tag{14}$$

which again includes a higher-level baseline accompanied by corrections for basis set incompleteness error,

$$\Delta C_{6,\text{basis}} = C_{6,\text{iso}}^{\text{LR-CC2/da5Z}} - C_{6,\text{iso}}^{\text{LR-CC2/daQZ}}, \tag{15}$$

as well as core electron contributions to $C_{6,\text{iso}}$,

$$\Delta C_{6,\text{core}} = C_{6,\text{iso}}^{\text{LR-CC2[FULL]/daCQZ}} - C_{6,\text{iso}}^{\text{LR-CC2/daQZ}}, \tag{16}$$

computed using the second-order approximate coupled cluster singles and doubles model (CC2).[116] Since the values of $\Delta C_{6,\text{basis}}$ and $\Delta C_{6,\text{core}}$ are essentially the same when computed with CC2 and CCSD, the more computationally tractable CC2 method was employed here.

Since the uncoupled HF (UCHF) dispersion energy contributes to the binding energy at the MP2 level,[117–120] and this energy contribution can be obtained using the corresponding dispersion coefficients at sufficiently large intermolecular distances, it is also of interest to compute $C_{6,\text{iso}}^{\text{MP2}}$ for comparative purposes. For the experimental equilibrium geometry, the $C_{6,\text{iso}}^{\text{MP2}}$ coefficients were obtained using the Casimir-Polder integral over the corresponding UCHF frequency-dependent polarizabilities (computed with the daQZ basis set). The Casimir-Polder integral was numerically evaluated using a Gauss-Chebyshev quadrature scheme.[121] Because of the symmetry properties associated with the trigonometric functions in the Gauss-Chebyshev scheme, it is sufficient to compute only $N_{\text{pts}}/2$ grid points for even values of N_{pts}. All C_6 calculations in this work used $N_{\text{pts}} = 40$ in order to obtain accurate and converged dispersion coefficients, although $N_{\text{pts}} = 20$ is usually more than sufficient for such purposes.

C. Vibrational contributions to α

The inclusion of vibrational contributions to α is essential for meaningful comparison to experiment.[18,36,37,54,122] According to Marti and Bishop,[123] the total vibrational (vib) contribution to α can be defined as

$$\alpha(\text{vib}) = \alpha^{\text{ZP}} + \alpha^{v}, \tag{17}$$

where α^{ZP} is the zero-point (ZP) correction and α^{v} is the so-called pure vibrational contribution. Adding $\alpha(\text{vib})$ to the electronic α described above allows us to compare our theoretical results with experimentally determined quantities measured at finite frequencies and/or extrapolated to the static limit. Since α^{v} is essentially negligible at such frequencies,[124] only α^{ZP} is required to obtain the vibrational contribution to α in this study. The method used herein to obtain the vibrational contribution to α is based on the scheme proposed by Russell and Spackman.[54] In their study, the "zero-point vibrational correction (ZPVC)" term is precisely the same as α^{ZP} in Eq. (17).[54] As such, α^{ZPVC} will be used to denote the zero-point vibrational corrections to α throughout this work.

To compute these vibrational corrections, we expand the potential energy V (in cm^{-1}) as a Taylor series in the dimensionless normal mode coordinates q_i as follows:

$$V = V_e + \frac{1}{2}\sum_i w_i q_i^2 + \frac{1}{6}\sum_{ijk}\phi_{ijk} q_i q_j q_k + \frac{1}{24}\sum_{ijkl}\phi_{ijkl} q_i q_j q_k q_l + \cdots. \tag{18}$$

In this expression, w_i are the harmonic (quadratic) vibrational frequencies, while ϕ_{ijk} and ϕ_{ijkl} are the anharmonic cubic and quartic force constants, respectively. The quantity V_e is evaluated at the (global) minimum of the PES, i.e., $r_1 = r_2 = r_e$ and $\theta = \theta_e$. The dimensionless normal mode coordinates q_i can be transformed into mass-weighted normal mode coordinates Q_i using the following equation:[125]

$$q_i = c_q w_i^{1/2} Q_i, \tag{19}$$

where w_i and Q_i have units of cm^{-1} and bohr $\mathrm{amu}^{1/2}$, respectively, and $c_q = 0.091\,136$ is the required conversion factor. We note in passing that the anharmonic cubic force constants ϕ_{ijk} in this work only differ from the k_{ijk} used by Nielsen[126] by simple numerical factors.[125]

For the ground vibrational state of water, α^{ZPVC} can be derived from first-order perturbation theory (by neglecting higher-order terms arising from anharmonic quartic force constants and cubic partial derivatives of α) and is given by[54,127,128]

$$\alpha^{\mathrm{ZPVC}} \approx \frac{1}{4}\sum_i \left\{ \left(\frac{\partial^2 \alpha}{\partial q_i^2}\right)_e - \sum_j \frac{\phi_{iij}}{w_j}\left(\frac{\partial \alpha}{\partial q_j}\right)_e \right\}. \tag{20}$$

In this expression, i and j run over the three vibrational modes of H_2O (which correspond to bending, symmetric stretching, and asymmetric stretching), while the $(\partial\alpha/\partial q_j)_e$ and $(\partial^2\alpha/\partial q_i^2)_e$ terms represent the first and second partial derivatives of α (with respect to a given normal mode) evaluated at the $r_1 = r_2 = r_e$ and $\theta = \theta_e$ geometry.

To compute α^{ZPVC} at the CCSDT/daTZ level, a numerical geometry optimization was first performed to locate the global minimum on the PES, followed by numerical calculation of the corresponding Hessian to obtain the harmonic vibrational frequencies and normal modes. A series of displaced geometries with respect to the CCSDT/daTZ structure (which has an OH bond length of $r_e = 0.9617$ Å and a HOH angle of $\theta_e = 104.1713°$) was then generated by taking displacements along each of the three normal modes in both the positive and negative directions with a step size of Δq. Along each of the i normal modes, there were six single displacements: $\{\pm\Delta q_i\}$, $\{\pm 2\Delta q_i\}$, and $\{\pm 3\Delta q_i\}$. Combinations of any two normal modes i and j were also included, which leads to 36 double displacements: $\{\pm\Delta q_i, \pm 2\Delta q_i, \pm 3\Delta q_i\}/\{\pm\Delta q_j, \pm 2\Delta q_j, \pm 3\Delta q_j\}$. Triple displacements were also necessary when calculating quartic force constants using the finite-difference scheme. Such displacements couple all three normal modes and require an additional 64 combinations: $\{\pm\Delta q_i, \pm 2\Delta q_i\}/\{\pm\Delta q_j, \pm 2\Delta q_j\}/\{\pm\Delta q_k, \pm 2\Delta q_k\}$. To ensure the accuracy of our finite-differencing scheme for numerical evaluation of the derivatives in Eq. (20), we also compared our results against a least-squares fit of these quantities and found negligible differences. With three normal modes, a total number of $6\times 3 + 36\times 3 + 64 = 190$ displaced geometries were considered in this work.

The Cartesian coordinates for a geometry with a displacement Δq_i along the normal mode coordinate q_i were obtained via[129]

$$\Delta x_n^{(i)} = c_x \gamma_i^{-1/2} l_{ni} M_n^{-1/2} \Delta q_i, \tag{21}$$

in which $\gamma_i = \lambda_i^{1/2}/\hbar$, λ_i and l_{ni} are the eigenvalues (in hartree bohr^{-2} amu^{-1}) and eigenvectors, respectively, of the mass-weighted Cartesian force constant matrix evaluated at the CCSDT/daTZ minimum, and $\Delta x_n^{(i)}$ denotes a Cartesian displacement (in bohr) of an atom n with mass M_n (in amu) along the normal mode i. In this expression, $c_x = 0.153\,042$ is the required conversion factor to obtain the displaced Cartesian coordinates Δx in bohr. Properties such as V and α were then computed for the CCSDT/daTZ minimum and displaced geometries thereof. All of the required derivatives in Eq. (20) were calculated using fourth-order central differences with a step size of $\Delta q = 0.130\,683$.

In order to compare our theoretical results with experiment, the total α must include both electronic and vibrational contributions, i.e.,

$$\begin{aligned}\alpha^{\mathrm{total}} &\approx \alpha + \alpha^{\mathrm{ZPVC}} \\ &= \alpha^{\mathrm{LR\text{-}CCSDT/daQZ}} + \Delta\alpha_{\mathrm{basis}} + \Delta\alpha_{\mathrm{core}} + \alpha^{\mathrm{ZPVC}},\end{aligned} \tag{22}$$

where $\alpha^{\mathrm{LR\text{-}CCSDT/daQZ}}$, $\Delta\alpha_{\mathrm{basis}}$, and $\Delta\alpha_{\mathrm{core}}$ were computed at the experimental equilibrium geometry using Eqs. (8)–(10) and α^{ZPVC} was computed at the CCSDT/daTZ optimized geometry using Eq. (20).

In this work, all CC calculations were performed using an in-house modified version of the tensor contraction engine (TCE) response-property module[130–132] contained in the NWChem (v6.6) software package,[133] except for the LR-CC calculations for the Cauchy moments,[113,114] which were carried out using Dalton2016.[134,135] All finite-field HF, MP2, and DFT calculations, as well as computations of UCHF polarizabilities and $C_{6,\mathrm{iso}}^{\mathrm{MP2}}$ dispersion coefficients, were performed using a locally modified version of Q-Chem.[136] A (75, 302) quadrature grid was used to evaluate the semi-local part of the DFT functionals and the SG-1 grid[137] was used for the non-local (VV10) correlation.[138]

III. RESULTS AND DISCUSSION

A. Geometric dependence of α in the DPS-H_2O-3K database

The main goal of this study is to unravel the geometric dependence of the α tensor of the H_2O molecule as well as provide an analytical formula for this quantity which can be used for the development (and assessment) of next-generation force fields and machine-learning based approaches for modeling water in complex condensed-phase environments. The reference data for the DPS-H_2O-3K database (computed at the LR-CCSDT/daTZ level of theory) employed in our fitting procedure are discussed first.

At the experimental equilibrium geometry ($r_0 = 0.9578$ Å and $\theta_0 = 104.4776°$, located in the xz-plane),[88] α is essentially isotropic with $\alpha_{\mathrm{aniso}} = 0.51$ bohr^3 and $\alpha_{xx} > \alpha_{zz} > \alpha_{yy}$, with $\alpha_{xx} = 9.98$ bohr^3, $\alpha_{zz} = 9.63$ bohr^3, $\alpha_{yy} = 9.40$ bohr^3, and $\alpha_{\mathrm{iso}} = 9.67$ bohr^3, as shown in Table I. However, the molecular geometries accessed in the condensed-phase are significantly different from the equilibrium geometry. For non-equilibrium bond lengths and angles, α becomes strongly anisotropic, with

TABLE I. Current benchmark values for the static dipole polarizability components (α_{xx}, α_{yy}, and α_{zz}) of the H_2O molecule at its experimental equilibrium geometry, as well as the corresponding isotropic (α_{iso}) and anisotropic (α_{aniso}) measures of this tensor. All values are provided in bohr^3.

Method	α_{xx}	α_{yy}	α_{zz}	α_{iso}	α_{aniso}
LR-CCSD/W6[a,b]	9.990	9.329	9.631	9.650	0.573
CCSD(T)/aTZ[c,d]	9.915	9.038	9.378	9.444	0.766
LR-CC3/daTZ+$\Delta CC^{Q/T}_{\text{basis}}$ [a,e,f]	9.890	9.260	9.540	9.560	0.540
CCSD(T)/CBS[c,g]	9.832	9.186	9.479	9.499	0.560
CCSDTQ(P)/CBS[c,g,h]	9.832	9.198	9.479	9.503	0.551
UCHF/daQZ[i]	7.823	6.288	7.298	7.136	1.352
LR-CCSDT/daTZ[a,i]	9.977	9.397	9.630	9.668	0.506
LR-CCSDT/daQZ[a,i]	9.928	9.311	9.583	9.608	0.535
LR-CCSDT/daQZ+$\Delta\alpha_{\text{basis}}$ [a,i,j]	9.906	9.276	9.557	9.579	0.547
LR-CCSDT/daQZ+$\Delta\alpha_{\text{basis}}$+$\Delta\alpha_{\text{core}}$ [a,i,j,k]	9.874	9.223	9.520	9.539	0.565

[a]Linear response calculation.
[b]Reference 37. r = 0.9584 Å and θ = 104.44°.
[c]Orbital-relaxed finite field calculation.
[d]Reference 44. CCSD(T)/aTZ optimization with r = 0.9589 Å and θ = 104.33°.
[e]Reference 36. r = 0.9570 Å and θ = 104.50°.
[f]$\Delta CC^{Q/T}_{\text{basis}}$ = LR-CCSD/daQZ –LR-CCSD/daTZ.
[g]Reference 41. CCSD(T)/CBS approximated by a three-point daQZ/da5Z/da6Z extrapolation.
[h]CCSDTQ(P)/CBS = CCSD(T)[FULL]/CBS + [CCSDTQ(P)/aDZ –CCSD(T)/aDZ].
[i]This work. Experimental geometry from Ref. 88 with $r = r_0$ = 0.9578 Å and $\theta = \theta_0$ = 104.4776°.
[j]$\Delta\alpha_{\text{basis}}$ = LR-CCSD/da5Z–LR-CCSD/daQZ; see Eq. (9).
[k]$\Delta\alpha_{\text{core}}$ = LR-CCSD[FULL]/daCQZ–LR-CCSD/daQZ; see Eq. (10).

α_{aniso} values as high as 10.66 bohr^3 for the geometry with $r_1 = r_2$ = 1.2980 Å and θ = 135°. Across the 3125 total (1625 symmetry-unique) geometries in this work, α_{iso} also has a quite extensive range, with observed values of 6.20–16.55 bohr^3 (i.e., 64%–171% of α_{iso} at the experimental equilibrium geometry), with diagonal components ranging from approximately 6-24 bohr^3 and a non-diagonal component (α_{xz}) ranging from approximately 0-4 bohr^3.[139] Among the diagonal components, we find that the largest geometric dependence occurs for α_{xx}, the in-plane component of α that is orthogonal to the C_2 molecular axis, which has the most extensive range of observed α values (5.60-23.63 bohr^3). This is followed by α_{zz} (the in-plane component along the C_2 molecular axis) and α_{yy} (the out-of-plane component), with ranges of 5.83-16.35 bohr^3 and 7.12-12.43 bohr^3, respectively. This observation is consistent with the fact that the polarizability is the strongest along the bonds and changing r_1, r_2, and θ will lead to the largest differences in the x- and z-components in the water molecule (Fig. 1).

Figure 2 shows the α dependence on the OH bond lengths by fixing $\theta = \theta_0$ = 104.4776°. As seen in the experimental equilibrium geometry, we also find that the diagonal components of α follow the trend that $\alpha_{xx} > \alpha_{zz} > \alpha_{yy}$, i.e., the in-plane components of α are larger than the out-of-plane component. As expected, all α components increase as the OH bond lengths are stretched. Both of these findings are consistent with the general proportionality relationship between α and molecular volume.[140] For reference, the full DPS-H_2O-3K database (Table S1) includes data for four additional HOH angles (θ = 75°, θ = 90°, θ = 120°, and θ = 135°) and the corresponding heat maps can be found in Figs. S1–S4. In varying θ from 75° to θ = 135°, it is clear from this database that changes in the OH bond lengths have a more significant impact on the α tensor.

B. Least-squares fit of the DPS-H_2O-3K database

To generate an accurate prediction of the DPS from the power series expansion formula in Eq. (2), all of the reference data contained in the DPS-H_2O-3K database were used to obtain the optimal set of expansion coefficients ($\varphi^{(uv)}_{ijk}$) for each non-zero polarizability component (α_{xx}, α_{yy}, α_{zz}, and α_{xz}). Table II lists all M = 35 of these coefficients (for an expansion up to order p = 4) obtained using the linear least-squares procedure outlined in Eq. (4) as well as a statistical analysis of the power series performance in reproducing each of these four components. Using this expansion order, we are able to reproduce the DPS of H_2O with high fidelity, as graphically shown in Fig. 3. Here we report negligible mean signed errors (MSEs) and conclude that our approach has no systematic error. Root-mean-square errors (RMSEs) for the α_{xx}, α_{yy}, α_{zz}, and α_{xz} components were quite small and computed as 0.0115, 0.0015, 0.0054, and 0.0048 bohr^3, respectively, across this extensive sample of non-equilibrium geometries. To put these errors into context, the corresponding relative RMSE values (defined as the ratio of the RMSE to the mean absolute value of the given reference quantity across the database) were computed as 0.10%, 0.02%, 0.05%, and 0.42%, respectively. This measure provides a consistent metric for evaluating the relative error in all four components of α (since α_{xz} takes on both positive and negative values), thereby illustrating the high accuracy and precision associated with this approach. For reference, the maximum errors (MAXEs) encountered for the α_{xx}, α_{yy}, α_{zz}, and α_{xz} components are 0.0663, 0.0094, 0.0335, and 0.0204 bohr^3, respectively. Despite the fact that relatively large geometric distortions have been sampled in this database, the largest MAXE (found for the α_{xx} component) corresponds to a deviation of only 0.3%.

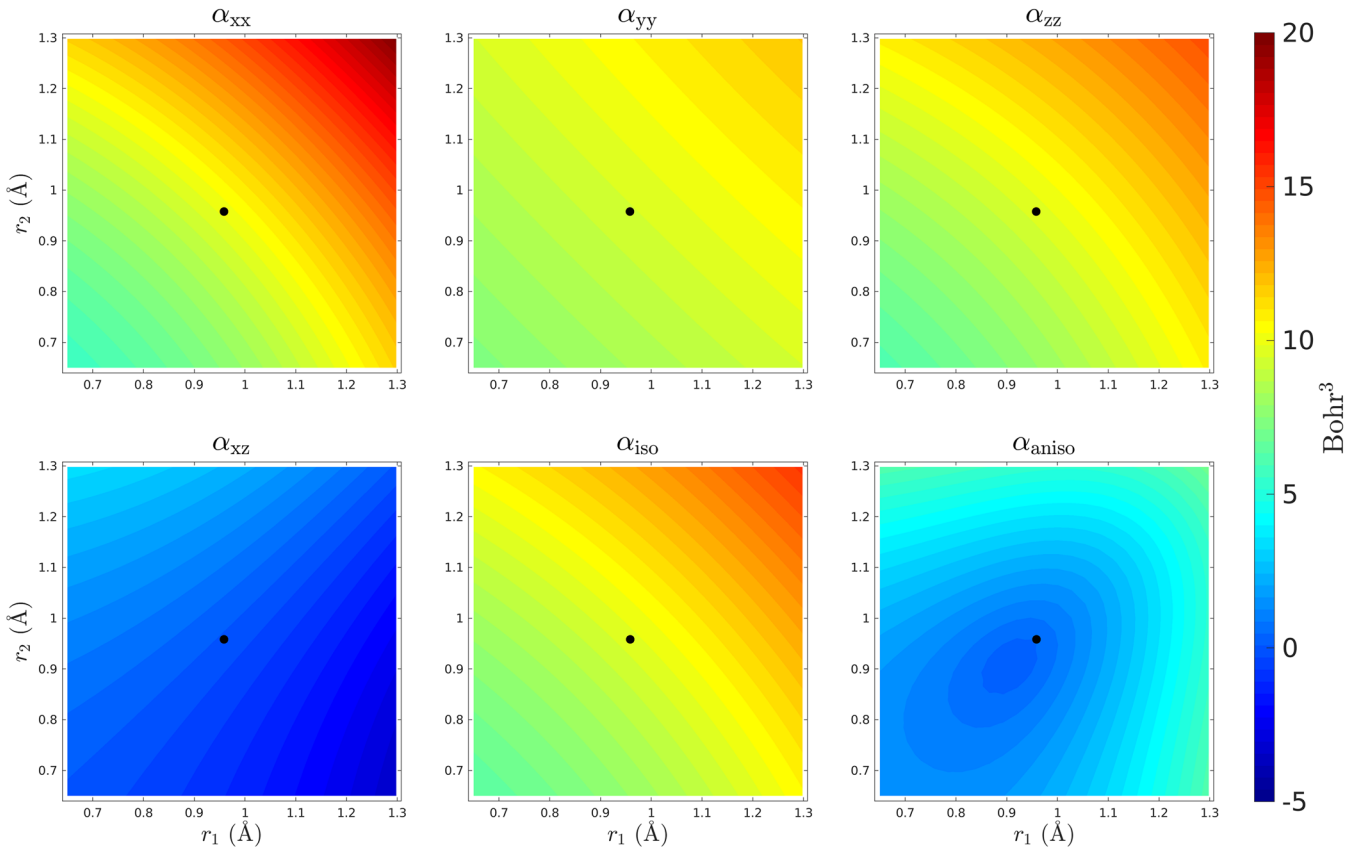

FIG. 2. Dipole polarizability surface (DPS) of H_2O as illustrated by heat maps of α_{xx}, α_{yy}, α_{zz}, α_{xz}, α_{iso}, and α_{aniso} computed at the LR-CCSDT/d-aug-cc-pVTZ level of theory for $N = 3125$ total (1625 symmetry-unique) geometries of the water molecule. All heat maps were obtained by varying the OH bond lengths (r_1 and r_2) at the fixed experimental HOH angle of $\theta = \theta_0 = 104.4776°$. The black spots in each heat map represent the location of the experimental equilibrium geometry (with $r_0 = 0.9578$ Å). The full DPS-H_2O-3K database (Table S1) includes data for four additional HOH angles ($\theta = 75°$, $\theta = 90°$, $\theta = 120°$, and $\theta = 135°$), and the corresponding heat maps can be found in Figs. S1–S4.

Such deviations can be further ameliorated by using a higher-order expansion (p = 5, 6) in Eq. (2), albeit at an increased computational cost (see Tables S3–S7 for the expansion coefficients corresponding to $p = 1, 2, 3, 5, 6$ and respective statistical error analyses). In doing so, we observe that all RMSE values are reduced by a factor of 3–5× and 11–15 × when the order is increased to $p = 5$ and $p = 6$, respectively. However, this is accompanied by an increase in the number of terms (M) in the expansion, i.e., from $M = 35$ ($p = 4$) to $M = 56, 84$ ($p = 5, 6$). Here one might argue that a power series expansion with $p = 4$ might already be too computationally demanding (and therefore impractical) for use during classical molecular dynamics (MD) simulations.[90] In this case, the $p = 3$ expansion (with $M = 20$) only leads to an increase of 3–4× in the RMSE values and may still be of sufficient accuracy for such purposes. Taking these issues into account, appropriate truncations of the power series expansion model presented in this work can be used to furnish an accurate and reliable analytical expression for the geometric dependence of the molecular polarizability of H_2O and can therefore be of potential use in the development of next-generation polarizable force fields for simulating condensed-phase aqueous properties such as the Raman spectra of liquid water.[141]

To utilize any of these expansion formulae to obtain the components of the polarizability tensor ($\overline{\alpha}$) in a water molecule that is in an arbitrary orientation, one simply needs to perform an orthogonal transformation (change of basis) on the polarizability tensor (α) corresponding to the same water molecule oriented according to the local reference frame defined in Fig. 1. This transformation is given by $\overline{\alpha} = R\,\alpha\,R^T$, in which R is the rotation matrix (obtained using the Kabsch algorithm[142] for instance) that transforms the Cartesian coordinates of the given water molecule into this reference orientation.

C. Basis set and core electron effects on α: The DPS-H_2O-25++ benchmark database

To further improve the DPS, we assembled a refined benchmark database that includes 25 symmetry-unique molecular geometries selected to span the more extensive DPS-H_2O-3K database. The polarizability values in this benchmark database (denoted as DPS-H_2O-25++) were computed according to the prescription in Eqs. (8)–(10) and therefore include both basis set effects and core electron corrections. Table III provides the tabulated data for the DPS-H_2O-25++ benchmark database (as well as the C6S-H_2O-25++ database, *vide infra*). The tabulated data for the corresponding refined V and μ can be found in Table S2.

We will first discuss the polarizability corresponding to the experimental equilibrium geometry of H_2O. In order to do so, we have compiled the current benchmark values for this

TABLE II. Power series expansion coefficients $\{\varphi_{ijk}\}$ up to order $p = 4$ in Eq. (2) for the non-zero components of the dipole polarizability tensor (α_{xx}, α_{yy}, α_{zz}, and α_{xz}) of H_2O. These expansion coefficients (denoted by 3K-FIT) were obtained via linear least-squares fitting of the DPS-H_2O-3K database (i.e., the dipole polarizability surface (DPS) computed for 3125 total (1625 symmetry-unique) geometries of the H_2O monomer at the LR-CCSDT/d-aug-cc-pVTZ level of theory). Statistical error analysis includes: the mean signed error (MSE), mean absolute error (MAE), root-mean-square error (RMSE), and maximum error (MAXE). Power series expansion coefficients (with corresponding statistical error analysis) for orders p = 1, 2, 3, 5, 6 that were obtained by fitting the DPS-H_2O-3K database can be found in Tables S3–S7.

i j k	α_{xx}	α_{yy}	α_{zz}	α_{xz}
0 0 0	9.9771	9.3966	9.3604	0.0000
1 0 0	2.7327	0.9375	−0.7384	0.0000
0 1 0	9.7668	3.4488	6.5935	−4.8375
0 0 1	9.7668	3.4488	6.5935	4.8375
0 1 1	6.2261	0.6858	−0.7018	0.0000
1 0 1	7.3665	0.6469	−5.1341	−2.7468
1 1 0	7.3665	0.6469	−5.1341	2.7468
2 0 0	0.8955	1.0923	2.6882	0.0000
0 2 0	7.9289	0.0879	3.7049	−5.1174
0 0 2	7.9289	0.0879	3.7049	5.1174
1 1 1	5.7822	1.5569	7.0468	0.0000
0 2 1	1.5136	−0.4588	−2.0099	−0.8873
2 0 1	−0.1568	1.0766	−0.1887	−5.0767
2 1 0	−0.1568	1.0766	−0.1887	5.0767
0 1 2	1.5136	−0.4588	−2.0099	0.8873
1 0 2	13.1882	0.0745	−6.8387	0.4035
1 2 0	13.1882	0.0745	−6.8387	−0.4035
3 0 0	−3.7738	0.0607	2.0610	0.0000
0 3 0	2.1964	−0.4605	−0.0562	−1.0425
0 0 3	2.1964	−0.4605	−0.0562	1.0425
2 1 1	5.7035	−2.4127	−7.0887	0.0000
1 2 1	−1.8827	−0.9577	0.2497	0.8875
1 1 2	−1.8827	−0.9577	0.2497	−0.8875
0 3 1	−5.1491	−0.3199	−0.9528	1.4800
3 0 1	−3.1781	1.8450	5.1037	−3.4654
3 1 0	−3.1781	1.8450	5.1037	3.4654
0 1 3	−5.1491	−0.3199	−0.9528	−1.4800
1 0 3	15.8031	−0.8990	0.1261	6.3588
1 3 0	15.8031	−0.8990	0.1261	−6.3588
0 2 2	0.1749	−0.1762	−2.0012	0.0000
2 0 2	2.7300	0.8422	2.1690	−4.7621
2 2 0	2.7300	0.8422	2.1690	4.7621
4 0 0	−3.7153	−0.2555	−1.9366	0.0000
0 4 0	−2.6692	−1.0953	−2.8224	2.0988
0 0 4	−2.6692	−1.0953	−2.8224	−2.0988
MSE	−0.0002	0.0000	0.0001	0.0000
MAE	0.0087	0.0011	0.0037	0.0031
RMSE	0.0115	0.0015	0.0054	0.0048
MAXE	0.0663	0.0094	0.0335	0.0204

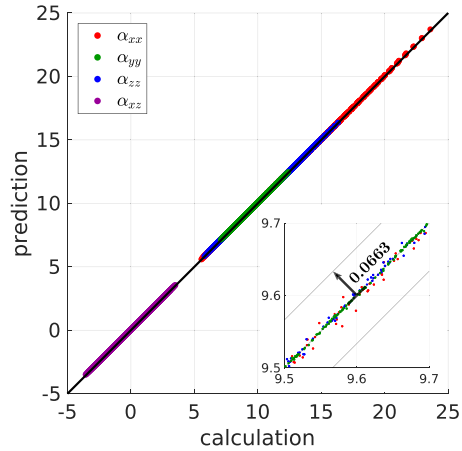

FIG. 3. Correlation plot for the non-zero components of the dipole polarizability tensor (α_{xx}, α_{yy}, α_{zz}, and α_{xz}) for the 3125 total (1625 symmetry-unique) geometries of the H_2O monomer in the DPS-H_2O-3K database. The predicted values for these quantities were obtained using the power series expansion in Eq. (2) with $p = 4$ and the coefficients provided in Table II. *Inset*: For near-equilibrium geometries, this power series expansion predicts α values with negligible error when compared to the largest MAXE observed in this database (i.e., 0.0663 bohr^3 for α_{xx} corresponding to a geometry far from equilibrium).

quantity from this work as well as an extensive survey of the literature (see Table I). In this work, the first improvement in the DPS-H_2O-25++ database is the baseline computation of α at the LR-CCSDT/daQZ level of theory, which results in a monotonic decrease in all non-zero components (α_{xx}, α_{yy}, and α_{zz}) when compared to LR-CCSDT/daTZ. This results in an overall decrease of 0.06 bohr^3 (−0.6%) in α_{iso} and a more substantial relative increase of 0.03 bohr^3 (+5.4%) in α_{aniso}. Further corrections for basis set incompleteness error via the $\Delta\alpha_{\text{basis}}$ correction defined in Eq. (9) provide an additional monotonic decrease in all non-zero components, yielding final values for α_{iso} and α_{aniso} that are smaller (by 0.03 bohr^3 or −0.3%) and larger (by 0.01 bohr^3 or +2.2%), respectively, when compared to the LR-CCSDT/daQZ results. These results not only demonstrate convergence of these values with respect to the basis set but also the trend to expect at the *true* complete basis set (CBS) limit: α_{iso} (α_{aniso}) will be slightly smaller (larger). Corrections for the use of the frozen-core approximation (in which only the valence electrons are accounted for in the electron correlation calculations) via the $\Delta\alpha_{\text{core}}$ correction defined in Eq. (10) are quite similar to the basis set corrections discussed above and are essentially additive. Here, we observe a further decrease in α_{iso} by 0.04 bohr^3 (−0.4%) and a further increase in α_{aniso} by 0.02 bohr^3 (+3.3%). By simultaneously accounting for both basis set incompleteness error and core electron contributions, our most reliable estimate for α_{iso} of H_2O at the experimental equilibrium geometry is 9.539 bohr^3 at the LR-CCSDT/daQZ + $\Delta\alpha_{\text{basis}}$ + $\Delta\alpha_{\text{core}}$ level of theory.

The most accurate and reliable results for α_{iso} from the literature are arguably given by Christiansen *et al.*[36] (9.560 bohr^3 using LR-CC3/daTZ + [LR-CCSD/daQZ–LR-CCSD/daTZ]) or Monten *et al.*[41] (9.503 bohr^3 using orbital-relaxed finite-field CCSD(T)[FULL]/CBS + [CCSDTQ(P)/aDZ–CCSD(T)/aDZ]). In addition, the data provided by the in-depth study of electron correlation and basis set effects in the calculation of α by Hammond *et al.*[11] can also be used to obtain a value of 9.576 bohr^3 using the LR-CCSDT/daQZ + [LR-CCSD/da5Z–LR-CCSD/daQZ] ≡ LR-CCSDT/daQZ + $\Delta\alpha_{\text{basis}}$ scheme advocated in this work. This quantity is in excellent agreement with our value of 9.579 bohr^3 computed at the same level of theory (albeit for a slightly different geometry). Based on the findings described above, we expect that the value obtained by Christiansen *et al.*[36] should be slightly overestimated, since higher-order basis set effects

TABLE III. Tabulated data comprising the DPS-H_2O-25++ and C6S-H_2O-25++ benchmark databases, which include values for the static dipole polarizability measures (α_{xx}, α_{yy}, α_{zz}, α_{xz}, $\alpha_{\rm iso}$, and $\alpha_{\rm aniso}$ in bohr^3) and isotropic dispersion coefficients ($C_{6,\rm iso}$ in hartree · bohr^6) for 25 symmetry-unique geometries of the H_2O molecule (with the experimental geometry in bold). As discussed in the main text, all static dipole polarizability values were computed at the LR-CCSDT/daQZ + $\Delta\alpha_{\rm basis}$ + $\Delta\alpha_{\rm core}$ level as defined in Eqs. (8)–(10). All isotropic dispersion coefficients were computed using the Casimir-Polder formula with frequency-dependent polarizabilities obtained via the Cauchy moment expansion at the level of LR-CCSD/daQZ + $\Delta C_{6,\rm basis}$ + $\Delta C_{6,\rm core}$ as described in Eqs. (14)–(16).

θ (°)	r_1 (Å)	r_2 (Å)	α_{xx}	α_{yy}	α_{zz}	α_{xz}	$\alpha_{\rm iso}$	$\alpha_{\rm aniso}$	$C_{6,\rm iso}$
75	0.650 00	0.650 00	5.5930	6.9894	5.7689	0.0000	6.1171	1.3173	23.2637
75	0.650 00	0.957 78	7.2526	8.0186	7.9401	1.2083	7.7371	2.2165	32.9981
75	0.957 78	0.957 78	9.2432	9.0497	9.8932	0.0000	9.3954	0.7653	44.8636
75	0.957 78	1.298 00	12.4100	10.2026	13.3868	2.3973	11.9998	5.0224	62.9962
75	1.298 00	1.298 00	16.2760	11.3361	16.2447	0.0000	14.6189	4.9243	84.8450
90	0.650 00	0.650 00	5.5310	7.0677	5.8651	0.0000	6.1546	1.3999	23.3237
90	0.650 00	0.957 78	7.3339	8.0638	7.8061	1.1502	7.7346	2.0928	32.9905
90	0.957 78	0.957 78	9.5275	9.1180	9.6756	0.0000	9.4404	0.5003	45.0619
90	0.957 78	1.298 00	13.3460	10.2845	12.7980	2.4157	12.1428	5.0500	63.8022
90	1.298 00	1.298 00	17.9249	11.4656	15.4889	0.0000	14.9598	5.6499	87.1397
104.4776	0.650 00	0.650 00	5.5454	7.1627	6.0435	0.0000	6.2505	1.4346	23.6861
104.4776	0.650 00	0.957 78	7.4826	8.1476	7.7714	1.0642	7.8005	1.9316	33.0731
104.4776	**0.957 78**	**0.957 78**	**9.8744**	**9.2233**	**9.5190**	**0.0000**	**9.5391**	**0.5646**	**45.5367**
104.4776	0.957 78	1.298 00	14.3620	10.4113	12.2721	2.3653	12.3485	5.3388	65.0146
104.4776	1.298 00	1.298 00	19.6494	11.6283	14.7074	0.0000	15.3284	7.0086	89.5852
120	0.650 00	0.650 00	5.6092	7.2768	6.3404	0.0000	6.4088	1.4478	24.3577
120	0.650 00	0.957 78	7.6733	8.2742	7.8569	0.9292	7.9348	1.6955	33.9099
120	0.957 78	0.957 78	10.2743	9.3831	9.4615	0.0000	9.7063	0.8547	46.4800
120	0.957 78	1.298 00	15.5167	10.6086	11.8255	2.2166	12.6503	5.8598	66.8574
120	1.298 00	1.298 00	21.5929	11.8713	13.9605	0.0000	15.8082	8.8636	92.8074
135	0.650 00	0.650 00	5.6928	7.3896	6.7188	0.0000	6.6004	1.4802	25.2707
135	0.650 00	0.957 78	7.8406	8.4215	8.0612	0.7476	8.1078	1.3909	34.8131
135	0.957 78	0.957 78	10.6233	9.5781	9.5352	0.0000	9.9122	1.0673	47.5680
135	0.957 78	1.298 00	16.5870	10.8734	11.5625	1.9477	13.0076	6.3689	68.9115
135	1.298 00	1.298 00	23.4689	12.2087	13.4404	0.0000	16.3727	10.6977	96.0676

(beyond LR-CCSD/daQZ) and core electron corrections *both* lead to a decrease in $\alpha_{\rm iso}$ (Table I). Although Monten *et al.*[41] accounted for core electron contributions to α, they utilized a three-point extrapolation based on CCSD(T)[FULL] calculations with the daQZ, da5Z, and da6Z basis sets, which do not explicitly include functions parameterized for describing core-valence interactions. Furthermore, the accuracy and reliability of their pairwise correction to account for electron correlation effects beyond CCSD(T) via CCSDTQ(P)/aDZ–CCSD(T)/aDZ, while a noteworthy and valiant effort, is very likely to be unreliable, since it has been demonstrated that the aDZ basis set is insufficient for converging higher-order correlation effects [even at the level of CCSD(T)–MP2].[143–145] In this regard, even the sign of the correction can be incorrect and Marshall *et al.*[146] have shown that basis sets of at least triple-ζ quality are necessary to capture higher-order electron correlation effects in a converged manner. With the increase in computational resources available today, we sidestep this issue by computing all polarizabilities at the baseline LR-CCSDT/daQZ level of theory in the DPS-H_2O-25++ database. Given these stringent basis set requirements (which become even more important for higher-order correlation methods based on N-tuply excited Slater determinants) and the prohibitive computational cost associated with CC calculations beyond CCSDT, we were unable to sufficiently ascertain how higher-order electron correlation effects (beyond full triples) will alter the values of quantities such as $\alpha_{\rm iso}$ and $\alpha_{\rm aniso}$ in the H_2O molecule. Based on the difference between $\alpha_{\rm iso}$ ($\alpha_{\rm aniso}$) at the LR-CCSDT/daQZ and LR-CCSD/daQZ levels of theory, which we have computed to be +0.01 bohr^3 (−0.05 bohr^3), we expect that higher-order electron correlation effects from coupled cluster theory including single, double, triple, and quadruple excitations (CCSDTQ) will be negligible for $\alpha_{\rm iso}$, while absolute convergence of $\alpha_{\rm aniso}$ might even require corrections beyond full quadruples.

The electronic contribution to the molecular polarizability in H_2O can also be semi-quantitatively estimated from dipole oscillator strength distributions (DOSDs) obtained from an analysis of experimental photo-absorption cross sections and refractive index data. Due to the non-negligible vibrational contributions to α (see Sec. III F), such estimates can only be considered as semi-experimental sources of information that are almost certainly not precise enough to serve as benchmark values for this quantity.[87] Most notably, the DOSD result of 9.642 ± 0.096 bohr^3 from Zeiss and Meath[147] has served as the benchmark value for the electronic contribution to α in H_2O for a wide range of electronic structure methods.[25,35,49] As discussed above, our estimate for this quantity at the LR-CCSDT/daQZ + $\Delta\alpha_{\rm basis}$ + $\Delta\alpha_{\rm core}$ level of theory is 9.539 bohr^3, which is approximately 0.1 bohr^3 (or 1%) smaller than the

DOSD result and sits just at the bottom of the uncertainty in this experimental estimate. Other results for α_{iso} derived from refractive index data include: 9.823 ± 0.098 bohr^3 from Cuthbertson,[82] 9.703 ± 0.097 bohr^3 from Newbound,[84] and 9.601 ± 0.096 bohr^3 from Barrell.[85] From these data and Table I, one immediately notices that the experimental estimates for this quantity are all larger than the most accurate theoretical values. As mentioned above, this discrepancy is most likely due to the fact that the experimental estimates for the electronic contribution to α (which is fairly straightforward to compute theoretically) still include some vibrational contributions to this quantity. Since these contributions are quite sizable and always serve to increase α_{iso}, this can possibly explain the discrepancy between experiment and theory. To ensure a fair and accurate comparison, vibrational contributions to α should be included in both the experimental and theoretical estimates for the *total* molecular polarizability (see Sec. III F).

For all of these reasons, we believe that our estimates of the non-zero components of the electronic contribution to the molecular α of water (as well as α_{iso} and α_{aniso}) for the 25 (equilibrium + non-equilibrium) geometries in the DPS-H_2O-25++ database, which simultaneously account for higher-order electron correlation effects, basis set incompleteness error, and core electron corrections, should be regarded as the most accurate and reliable benchmarks for these quantities available to date. Similar to what we found above for the experimental equilibrium geometry, corrections for both basis set incompleteness error and core electron corrections via $\Delta\alpha_{\text{basis}}$ and $\Delta\alpha_{\text{core}}$ always lead to reductions in α_{iso} [by 0.03 bohr^3 (−0.3%) and 0.04 bohr^3 (−0.4%) on average, respectively] across these 25 geometries. Corrections to α_{aniso} are more difficult to quantify as both effects can lead to signed changes in this quantity across the database. In this regard, we find that basis set and core electron corrections lead to mean absolute deviations (mean absolute percent deviations) of 0.008 bohr^3 (+0.6%) and 0.015 bohr^3 (+0.9%), respectively, across the DPS-H_2O-25++ database. When the sign of these corrections are taken into account, these values are reduced to +0.1% and +0.2%. This is indicative that these corrections are almost equally distributed in sign across the database and that both corrections tend to slightly increase α_{aniso} on average. Another interesting point to note here is that the largest changes in α_{aniso} due to basis set and core electron corrections are neither found in the most non-equilibrium geometries nor the C_s geometries [in which α_{aniso} depends on the non-zero off-diagonal α_{xz} component; see Eq. (12)]. In fact, the largest corrections were found for two C_{2v} geometries: the experimental equilibrium geometry ($r_1 = r_2 = r_0 = 0.9578$ Å and $\theta = \theta_0 = 104.4776°$) and a neighboring geometry with $r_1 = r_2 = r_0$ and $\theta = 90°$. Here, we find basis set corrections of +2.0% and +2.2% and core electron corrections of +3.2% and +3.5% to α_{aniso}, respectively. These findings are strongly indicative that α_{aniso}—which describes the relative spatial distribution of the values in the α tensor—is a quite delicate measure of this response property that requires a simultaneous treatment of high-order electron correlation effects, basis set incompleteness error, and core electron corrections for sufficient convergence.

D. Performance of QC and DFT methods on the DPS-H_2O-25++ benchmark database

We now focus our discussion on the use of the DPS-H_2O-25++ benchmark database to assess the performance of a number of QC and DFT methodologies in the prediction of α across these 25 select geometries of the H_2O molecule. In order to do so, we computed these quantities for HF, MP2, and a wide range of DFT functionals using the orbital-relaxed finite-field method and the daQZ basis set, as shown in Table IV. For reference, we have also included LR-CCSD with the same basis set as well as the predictions from the power series expansion (up to order $p = 4$) in Eq. (2) based on least-squares fits of the more extensive DPS-H_2O-3K database (denoted by 3K-FIT).

As expected, the mean-field HF approximation tends to overestimate the HOMO–LUMO gap in molecules and therefore substantially underestimates the α components, resulting in unacceptably large RMSE values. MP2 performs much

TABLE IV. Root-mean-square errors (RMSE) associated with several QC methodologies and a wide range of DFT functionals in predicting all static dipole polarizability measures (α_{xx}, α_{yy}, α_{zz}, α_{xz}, α_{iso}, and α_{aniso} in bohr^3) of the 25 molecular geometries in the DPS-H_2O-25++ benchmark database. Unless otherwise specified, all QC and DFT calculations were performed using the orbital-relaxed finite-field method and the daQZ basis set. As described in the main text, the reference data for α were computed at the LR-CCSDT/daQZ + $\Delta\alpha_{\text{basis}}$ + $\Delta\alpha_{\text{core}}$ [Eqs. (8)–(10)] levels of theory. For reference, the final row (3K-FIT) contains the prediction from the power series expansion in Eq. (2) with $p = 4$ based on least-squares fits of the DPS-H_2O-3K database. For ease of comparison, the lowest three RMSE values in each column (excluding CCSD and 3K-FIT) have been highlighted in bold font.

Method	α_{xx}	α_{yy}	α_{zz}	α_{xz}	α_{iso}	α_{aniso}
HF	0.5814	1.3738	0.8120	0.2065	0.8172	1.1554
MP2	0.4565	0.3810	0.2352	0.1492	**0.1243**	0.7520
CCSD[a]	0.0735	0.0491	0.0703	0.0042	0.0635	0.0250
UCHF[b]	2.6461	3.0845	2.1319	0.1413	2.5775	0.8343
MP2*[c]	2.4840	2.9795	2.0033	0.8539	2.4423	0.8489
LSDA	0.7751	1.4340	1.0444	0.0401	1.0817	0.4839
BLYP	0.6158	1.3093	0.9086	0.0534	0.9390	0.5432
PBE	0.6024	1.3555	0.9672	0.0710	0.9645	0.6409
B3LYP	0.3390	0.5110	0.4177	0.0288	0.4153	0.1972
PBE0	**0.1736**	0.2782	0.2094	**0.0231**	0.2083	**0.1613**
M11	0.3327	0.3148	**0.1590**	0.0470	0.2530	0.2273
MN15	0.2241	**0.1801**	**0.1863**	0.0465	**0.1492**	0.2589
B97-2	**0.1526**	0.2700	0.1952	**0.0214**	0.1954	**0.1531**
ωB97X-D	0.1901	0.3710	0.2501	0.0261	0.2531	0.2260
B97M-V	0.5356	0.6776	0.4992	0.0674	0.5497	0.3157
ωB97X-V	0.2227	0.3257	0.2334	0.0318	0.2440	0.2011
ωB97M-V	0.3628	0.5343	0.4208	0.0314	0.4306	0.2112
MS2	0.5196	0.6419	0.5110	0.0795	0.5302	0.3551
MS2h	0.3828	0.3789	0.3086	0.0831	0.3104	0.3758
MVS	0.4492	**0.1547**	0.2112	0.0935	0.2221	0.4418
MVSh	0.5699	0.5231	0.4853	0.0573	0.5207	0.1850
SCAN	0.2376	0.5675	0.4153	0.0295	0.4009	0.2802
SCAN0	**0.1348**	**0.2186**	**0.0799**	0.0356	**0.1224**	0.1934
mBEEF	0.1568	0.3043	0.2634	**0.0239**	0.2347	**0.1400**
3K-FIT	0.1086	0.1724	0.1646	0.0073	0.0479	0.1333

[a]Linear response calculation.
[b]Field-free uncoupled HF calculation.
[c]Orbital-unrelaxed finite-field calculation.

better than HF and yields the second-best prediction for α_{iso} among all of the methods (excluding CCSD and 3K-FIT) in Table IV. Here we note that this agreement in α_{iso} is largely fortuitous, as the RMSE values for α_{xx}, α_{yy}, α_{zz}, α_{xz}, and α_{aniso} are still quite large at the MP2 level. Even worse results are obtained with MP2* (i.e., finite-field MP2 without orbital relaxation), thereby indicating that orbital relaxation should be included at the MP2 level to obtain reasonably accurate results. Not surprisingly, LR-CCSD/daQZ is able to outperform HF, MP2, and all of the DFT functionals considered herein by a sizable margin across the board. In the same breath, the analytical and closed-form 3K-FIT expression (which is based on LR-CCSDT/daTZ values for α) fares exceptionally well for all quantities of interest and outperforms HF, MP2, and almost all DFT functionals. What is quite interesting here is the observation that LR-CCSD/daQZ noticeably outperforms 3K-FIT (with the single exception of α_{iso}, where LR-CCSD/daQZ and 3K-FIT both have very small RMSE values), which highlights the importance of basis set incompleteness error over higher-order electron correlation (and even core electron corrections) in obtaining sufficiently accurate estimates for α in H_2O. We note in passing that higher-order truncations ($p = 5$, 6) of the power series expansion in Eq. (2) provide very little improvement over $p = 4$ in predicting α in the DPS-H_2O-25++ benchmark database.

The popular hybrid functional B3LYP does not perform well during calculations of α. By contrast, the PBE0 hybrid functional landed among the top three performers (excluding CCSD and 3K-FIT) in predicting α_{xx}, α_{xz}, and α_{aniso}. Although M11 and ωB97X-D have been recommended for calculating dipole polarizabilities,[25,41] their performance on these benchmark databases was not remarkable when compared to the other functionals tested (although it should be noted that M11 did perform well for α_{zz}). B97-2 has also been recommended[26] to obtain accurate α values, and it does indeed place among the top three (again excluding CCSD and 3K-FIT) in the prediction of α_{xx}, α_{xz}, and α_{aniso}, as found above for PBE0. However, the performance of both PBE0 and B97-2 is less satisfactory in describing the out-of-plane (α_{yy}) and in-plane (α_{zz}) components (and hence α_{iso}). In direct contrast to PBE0 and B97-2, the most up-to-date Minnesota functional (MN15) performs well for α_{yy}, α_{zz}, and α_{iso} quantities, but struggles with α_{xx}, α_{xz}, and α_{aniso}. Although the non-local B97M-V, ωB97X-V, and ωB97M-V functionals recently developed by Mardirossian and Head-Gordon perform quite well for a number of different systems,[104–106,148–150] these functionals do not excel in the prediction of α. This finding is consistent with the recent work by Hait and Head-Gordon,[151] which found that ωB97M-V is somewhat lacking in the prediction of polarizabilities. The MS2, MS2h, MVS, MVSh, and SCAN functionals developed by Perdew and co-workers do not perform better than the popular PBE0 functional. However, the SCAN0 functional, which is the hybrid version of SCAN proposed by Hui and Chai, performs very well for all α components and is the most reliable DFT method for calculating α in H_2O (see Table IV). Similar to PBE0 and B97-2, the mBEEF functional, which is based on the Bayesian error estimation functional framework, provides competitive results for some (but not all) α measures.

In summary, we find that the SCAN0 hybrid *meta*-GGA is the best DFT functional for computing the molecular α in H_2O, while PBE0, B97-2, and MN15 are comparable (among themselves) and still perform well. As such, it seems that some non-local HF exchange is essential to obtain sufficiently accurate α values in this molecule. All things considered, we recommend further investigation into the use of SCAN0, PBE0, B97-2, and MN15 for the calculation of small-molecule dipole polarizabilities.

E. Basis set and core electron effects on the C_6 dispersion coefficient: The C6S-H_2O-25++ benchmark database

Leading-order isotropic dispersion coefficients ($C_{6,\text{iso}}$) for these 25 representative geometries were obtained via numerical integration of the Casimir-Polder integral in Eq. (13) over the frequency-dependent isotropic dipole polarizabilities in the imaginary-frequency domain. As discussed in Sec. II B, the set of $\alpha_{\text{iso}}(i\omega)$ required for computing $C_{6,\text{iso}}$ were obtained via the Cauchy moment expansion at the LR-CC level of theory.[113,114] The final $C_{6,\text{iso}}$ values in our benchmark database (denoted as C6S-H_2O-25++) were computed according to the $C_{6,\text{iso}} = C_{6,\text{iso}}^{\text{LR-CCSD/daQZ}} + \Delta C_{6,\text{basis}} + \Delta C_{6,\text{core}}$ prescription given in Eqs. (14)–(16), which again includes both basis set effects and core electrons corrections. Since the values of $\Delta C_{6,\text{basis}}$ and $\Delta C_{6,\text{core}}$ are obtained by integrating over $\alpha_{\text{iso}}(i\omega)$, there are negligible differences between the use of the CCSD and CC2 models; as such, we have employed the more computationally tractable CC2 method for obtaining these corrections. Due to the underlying dependence on α, we stress here that the use of double augmentation in conjunction with high angular momentum in the underlying basis set is essential for obtaining accurate and converged C_6 dispersion coefficients.[42] For reference, the tabulated data for the C6S-H_2O-25++ benchmark database are provided in Table III.

We will first discuss the $C_{6,\text{iso}}$ dispersion coefficient corresponding to the experimental equilibrium geometry of H_2O. In order to do so, we have again compiled the current values for this quantity from this work as well as an extensive survey of the literature (see Table V). In this work, the baseline computation of $C_{6,\text{iso}}$ in the DPS-H_2O-25++ database is at the LR-CCSD/daQZ level of theory. For comparative purposes, we have also computed this quantity at the LR-CCSD/daTZ level, from which we observe that the higher-quality daQZ estimate leads to a reduction in $C_{6,\text{iso}}$ by 0.43 Hartree · bohr^6 or −0.9%. Further treatment of basis set incompleteness error via the $\Delta C_{6,\text{basis}}$ correction defined in Eq. (15) provides an additional decrease of 0.22 Hartree · bohr^6 or −0.5%. In analogy to the results for α_{iso} discussed in Sec. III C, these results not only demonstrate a very similar convergence of $C_{6,\text{iso}}$ with respect to basis set but also that $C_{6,\text{iso}}$ is expected to be slightly smaller at the fully converged CBS limit. Core electron contributions were estimated using the $\Delta C_{6,\text{core}}$ correction defined in Eq. (16) and are again quite similar to that found for α_{iso} above. In other words, this correction leads to a further reduction of 0.28 Hartree · bohr^6 (−0.6%), which is on the same order as the basis set correction for $C_{6,\text{iso}}$ and essentially additive. By simultaneously accounting for both

TABLE V. Current values for the leading-order isotropic dispersion coefficient ($C_{6,\mathrm{iso}}$ in Hartree · bohr^6) of the H_2O molecule at its experimental equilibrium geometry. Errors (in %) are with respect to the semi-quantitative experimental dipole oscillator strength distribution (DOSD) estimate of Zeiss and Meath.[147] Time-dependent methods are denoted by TD, and SP-aQZ is a modified version of the aQZ basis set to improve convergence of the dispersion energy.[156,157] See the main text for more details regarding the methods employed below.

Method	$C_{6,\mathrm{iso}}$	Error
TD-HF/daQZ[a]	39.63	−12.7
TD-PBE/daQZ[a]	50.50	11.3
TD-PBE0/daQZ[a]	45.83	1.0
SDT-MBPT(2)/[10s7p4d3f1g/7s3p3d1f][b]	46.44	2.4
TD-MP2[FULL]/SP-aQZ[c]	48.00	5.8
TD-CCSD[FULL]/SP-aQZ[c,d]	45.60	0.5
CCSD(3)/daQZ[a,e]	47.23	4.1
CCSD(3)/da5Z[e,f]	46.88	3.3
UCHF/daQZ[g,h]	41.04	−9.5
LR-CCSD/daTZ[g]	46.47	2.4
LR-CCSD/daQZ[g]	46.04	1.5
LR-CCSD/daQZ+$\Delta C_{6,\mathrm{basis}}$[g,i]	45.82	1.0
LR-CCSD/daQZ+$\Delta C_{6,\mathrm{basis}}$+$\Delta C_{6,\mathrm{core}}$[g,i,j]	45.54	0.4
DOSD	45.37	...

[a]Reference 42. r = 0.9584 Å and θ = 104.45°.
[b]Reference 13. r = 0.9572 Å and θ = 104.52°. Double perturbation theory with SDT contributions to second order.
[c]Reference 23. r = 0.9716 Å and θ = 104.69°.
[d]Orbital-relaxed spin-unrestricted calculation.
[e]Third-order CCSD polarization propagator method.
[f]Reference 152. r = 0.9576 Å and θ = 104.29°.
[g]This work. Experimental geometry from Ref. 88 with $r = r_0$ = 0.9578 Å and $\theta = \theta_0$ = 104.4776°.
[h]Field-free uncoupled HF calculation.
[i]$\Delta C_{6,\mathrm{basis}}$ = LR-CC2/da5Z–LR-CC2/daQZ; see Eq. (15).
[j]$\Delta C_{6,\mathrm{core}}$ = LR-CC2[FULL]/daCQZ-LR-CC2/daQZ; see Eq. (16).

basis set incompleteness error and core electron contributions, our most reliable result for the $C_{6,\mathrm{iso}}$ dispersion coefficient of H_2O at the experimental equilibrium geometry is 45.54 Hartree · bohr^6 at the LR-CCSD/daQZ+$\Delta C_{6,\mathrm{basis}}$+$\Delta C_{6,\mathrm{core}}$ level of theory. As a final sanity check, we note that the static-limit Cauchy moment, $S(-2)$, is equivalent to the static dipole polarizability and yields an α_{iso} value of 9.518 bohr^3 at the LR-CCSD/daQZ+$\Delta C_{6,\mathrm{basis}}$+$\Delta C_{6,\mathrm{core}}$ level. This value is only 0.2% smaller than α_{iso} at our benchmark level of LR-CCSDT/daQZ+$\Delta\alpha_{\mathrm{basis}}$+$\Delta\alpha_{\mathrm{core}}$ [see Eqs. (8)–(10)] and therefore serves as a highly accurate zero-frequency starting point for the evaluation of the Casimir-Polder integral.

Our $C_{6,\mathrm{iso}}$ result for H_2O at the experimental geometry is compared against values from semi-quantitative DOSD data[147] as well as other theoretical studies[13,23,40,42,152] in Table V (albeit at slightly different geometries). For the molecular $C_{6,\mathrm{iso}}$ of H_2O, the DOSD-based value of 45.37 Hartree · bohr^6 provided by Zeiss and Meath in 1977[147] has been taken as the reference for decades now. In this regard, we remind the reader of the uncertainties associated with the DOSD approach regarding the value for the *purely* electronic contribution to α_{iso},[87] where the presence of non-negligible vibrational contributions is difficult (if not impossible) to completely decouple from the electronic contributions without some additional theoretical input. In this work, we will use this semi-experimental measure of $C_{6,\mathrm{iso}}$ to compute the percent errors associated with all of the theoretical results listed in Table V and believe that our $C_{6,\mathrm{iso}}$ results at the level of LR-CCSD/daQZ+$\Delta C_{6,\mathrm{basis}}$+$\Delta C_{6,\mathrm{core}}$ can also serve as reliable benchmarks for this quantity.

As seen in Table V, TD-HF and TD-DFT (employing the PBE and PBE0 functionals) have been used to compute $C_{6,\mathrm{iso}}$ for the water molecule with the daQZ basis set.[42] While both TD-HF and TD-PBE make substantial errors in the prediction of $C_{6,\mathrm{iso}}$ for H_2O (i.e., −12.7% and +11.3%, respectively), the TD-PBE0 approach yields a $C_{6,\mathrm{iso}}$ dispersion coefficient within 1.0% of the DOSD value. These findings are consistent with the fact that HF (PBE) tends to overestimate (underestimate) the HOMO–LUMO gap in molecules. In this case, the PBE0 functional, which includes an admixture of exact (HF) exchange, leads to a very favorable (although certainly fortuitous) interpolation between these two results. Calculations of this quantity at the SDT-MBPT(2)[13] and TD-MP2[23] levels overestimate the DOSD value by 2.4% and 5.8%, respectively, while orbital-relaxed spin-unrestricted TD-CCSD[23] furnishes a $C_{6,\mathrm{iso}}$ coefficient with a deviation of only +0.5%. However, the convergence of the TD-MP2 and TD-CCSD results will require further investigation, since all electrons were active in these two calculations despite the use of valence-only Dunning basis sets. Use of the CCSD(3) polarization propagator method[152] combined with the daQZ[42] and da5Z[152] basis sets still overestimates the DOSD value by 4.1% and 3.3%, respectively. These results quite clearly demonstrate that basis set effects (even beyond quadruple-ζ) still make a noticeable contribution during molecular C_6 calculations. LR-CCSD calculations performed in this work yielded errors of +2.4% and +1.5% using the daTZ and daQZ basis sets, respectively. This error can be further reduced to +1.0% by employing the $\Delta C_{6,\mathrm{basis}}$ correction to account for basis set incompleteness error and even further reduced to 0.4% by sequentially adding the $\Delta C_{6,\mathrm{core}}$ correction for core electrons effects. As such, our LR-CCSD/daQZ+$\Delta C_{6,\mathrm{basis}}$+$\Delta C_{6,\mathrm{core}}$ scheme predicts a $C_{6,\mathrm{iso}}$ dispersion coefficient for the H_2O molecule that is within +0.4% of the DOSD value and is arguably the most accurate among all of the theoretical methods listed in Table V.

Since the UCHF dispersion energy contributes to the binding energy at the MP2 level,[117–120] we have also computed the corresponding $C_{6,\mathrm{iso}}^{\mathrm{MP2}}$ dispersion coefficient for H_2O via the Casimir-Polder integral over UCHF frequency-dependent polarizabilities. Here we find that $C_{6,\mathrm{iso}}^{\mathrm{MP2}}$ = 41.04 Hartree · bohr^6 using the daQZ basis set, which substantially underestimates the DOSD value by −9.5%. This finding is consistent with the corresponding value of 7.14 bohr^3 for $\alpha_{\mathrm{iso}}^{\mathrm{UCHF}}$, which underestimates our benchmark value for this quantity by over 25% (see Table I). We note in passing that this trend of underestimating both α_{iso} and $C_{6,\mathrm{iso}}$ is not universal. In the case of the benzene molecule, for example, we find that $\alpha_{\mathrm{iso}}^{\mathrm{UCHF}}$ = 67.40 bohr^3 at the UCHF/aDZ//B97M-V/aDZ level, which is only 2% less than the LR-CCSD/aDZ value of 68.87 bohr^3. By contrast, however, the corresponding $C_{6,\mathrm{iso}}^{\mathrm{MP2}}$ for benzene is 2366.97 Hartree · bohr^6, which is more than 30% larger than the LR-CCSD/aDZ value of 1817.00 Hartree · bohr^6. This discrepancy largely originates from the frequency dependence of this quantity and will be the subject of a future publication.

We conclude this section with a brief discussion of the trends observed across the 25 geometries that comprise the C6S-H_2O-25++ database (see Table III). As found above for α_{iso}, we note that the range of $C_{6,\text{iso}}$ values encountered when changing the bond lengths and angles in the H_2O molecule is quite remarkable and spans 23.3-96.1 Hartree · bohr^6. In this regard, we find that these values follow a similar trend to α, in which molecular geometries with reduced volumes (shorter bond lengths and smaller angles) have substantially lower $C_{6,\text{iso}}$ dispersion coefficients than molecular geometries with increased volumes (longer bond lengths and larger angles). Since $C_6 \propto \alpha^2$ and $\alpha \propto V$, our findings are again consistent with our intuition for this quantity.[140]

F. Zero-point vibrational contributions to α

As discussed in Secs. II C and III C, the vibrational contribution to α can be quite sizable and must be included in both the experimental and theoretical estimates for the *total* molecular polarizability to ensure a fair and accurate comparison.[18,36,37,54,122] In order to compute the zero-point vibrational contributions (ZPVCs) to α (namely, α^{ZPVC}) for the H_2O molecule in its ground vibrational state, one needs to calculate the force constants and normal mode derivatives required to evaluate Eq. (20). To calculate these quantities, we first performed a numerical geometry optimization at the CCSDT/daTZ level of theory to obtain the geometry ($r_1 = r_2 = r_e = 0.9617$ Å and $\theta = \theta_e = 104.1713°$) and a subsequent vibrational frequency (Hessian) analysis to obtain the corresponding normal modes [bending (q_1), symmetric stretching (q_2), and asymmetric stretching (q_3)]. Using these normal modes, we then computed the harmonic (quadratic) force constants as well as all anharmonic (cubic and quartic) force constants for the H_2O molecule [as defined in Eq. (18)] via a fourth-order central difference scheme (see Table VI). The first and second derivatives of α (with respect to the dimensionless normal mode coordinates), which are related to the intensities of the Raman overtone bands,[153] were also calculated using fourth-order central differences at the LR-CCSDT/daTZ level (see Table VII). To demonstrate the accuracy and precision associated with the fourth-order central difference scheme employed herein, we compared the harmonic force constants in Table VI with the vibrational frequencies obtained from diagonalizing the numerically computed Hessian matrix (which yielded values of 1648.11, 3810.84, and 3918.69 cm^{-1} for ω_1, ω_2, and ω_3, respectively). Here, we find that the maximum deviation is only 0.38 cm^{-1} (or 0.01%), which we take as negligible in magnitude and a stringent cross-validation of our numerical approach.

As summarized in Table VIII, α^{ZPVC} has also been studied in the H_2O molecule using a wide range of theoretical methods. Using the CCSDT/daTZ scheme outlined in this work, we find that $\alpha^{\text{ZPVC}}_{\text{iso}}$ and $\alpha^{\text{ZPVC}}_{\text{aniso}}$ are given by 0.2916 and 0.2693 bohr^3,

TABLE VI. Harmonic (quadratic) and anharmonic (cubic and quartic) force constants (in cm^{-1}) for the H_2O molecule computed at the CCSDT/daTZ level of theory. All force constants were defined according to Eq. (18) and numerically calculated using a fourth-order central difference scheme. The bending, symmetric stretching, and asymmetric stretching vibrational (normal) modes are indexed by 1, 2, and 3, respectively.

Quantity	Value
ω_1	1647.9918
ω_2	3811.0479
ω_3	3919.0733
ϕ_{111}	−255.4522
ϕ_{222}	−1803.4644
ϕ_{333}	0.0000
ϕ_{112}	306.2171
ϕ_{122}	71.4797
ϕ_{113}	0.0000
ϕ_{133}	265.8201
ϕ_{223}	0.0000
ϕ_{233}	−1805.1280
ϕ_{123}	0.0000
ϕ_{1111}	−77.5100
ϕ_{2222}	663.0970
ϕ_{3333}	651.4556
ϕ_{1112}	148.4140
ϕ_{1113}	0.0000
ϕ_{1122}	−367.4915
ϕ_{1133}	−386.2881
ϕ_{1123}	0.0000
ϕ_{1222}	−63.0792
ϕ_{1333}	0.0000
ϕ_{1223}	0.0000
ϕ_{1233}	−123.3426
ϕ_{2223}	0.0000
ϕ_{2233}	718.1562
ϕ_{2333}	0.0000

TABLE VII. First and second derivatives (in a.u.) of α (with respect to the dimensionless normal mode coordinates) in the H_2O molecule computed at the LR-CCSDT/daTZ level. All derivatives were numerically calculated using a fourth-order central difference scheme. The bending, symmetric stretching, and asymmetric stretching vibrational (normal) modes are indexed by 1, 2, and 3, respectively. All derivatives of α that are not shown below are zero.

Quantity	Value
$(\partial\alpha_{xx}/\partial q_1)_e$	0.185 234
$(\partial\alpha_{xx}/\partial q_2)_e$	1.397 540
$(\partial\alpha_{yy}/\partial q_1)_e$	0.061 399
$(\partial\alpha_{yy}/\partial q_2)_e$	0.488 074
$(\partial\alpha_{zz}/\partial q_1)_e$	−0.191 194
$(\partial\alpha_{zz}/\partial q_2)_e$	0.935 593
$(\partial\alpha_{xz}/\partial q_3)_e$	−0.690 219
$(\partial^2\alpha_{xx}/\partial q_1^2)_e$	0.239 266
$(\partial^2\alpha_{xx}/\partial q_2^2)_e$	0.222 397
$(\partial^2\alpha_{xx}/\partial q_3^2)_e$	0.105 479
$(\partial^2\alpha_{xx}/\partial q_1\partial q_2)_e$	0.082 915
$(\partial^2\alpha_{yy}/\partial q_1^2)_e$	0.113 416
$(\partial^2\alpha_{yy}/\partial q_2^2)_e$	0.008 454
$(\partial^2\alpha_{yy}/\partial q_3^2)_e$	−0.014 778
$(\partial^2\alpha_{yy}/\partial q_1\partial q_2)_e$	0.002 844
$(\partial^2\alpha_{zz}/\partial q_1^2)_e$	0.251 904
$(\partial^2\alpha_{zz}/\partial q_2^2)_e$	0.066 170
$(\partial^2\alpha_{zz}/\partial q_3^2)_e$	0.065 265
$(\partial^2\alpha_{zz}/\partial q_1\partial q_2)_e$	−0.086 027
$(\partial^2\alpha_{xz}/\partial q_1\partial q_3)_e$	0.051 429
$(\partial^2\alpha_{xz}/\partial q_2\partial q_3)_e$	−0.101 449

TABLE VIII. Current values (in bohr^3) for the zero-point vibrational correction (ZPVC) to the isotropic ($\alpha_{\rm iso}^{\rm ZPVC}$) and anisotropic ($\alpha_{\rm aniso}^{\rm ZPVC}$) measures of the dipole polarizability for a H_2O molecule in its ground vibrational state. When available at the same level of theory (unless otherwise specified), we also provide the values of the electronic contributions to $\alpha_{\rm iso}$ and $\alpha_{\rm aniso}$, the relative percentages of the vibrational corrections to the electronic contributions in each of these quantities ($\eta_{\rm iso}$ and $\eta_{\rm aniso}$), and $\alpha_{\rm iso}^{\rm total} = \alpha_{\rm iso} + \alpha_{\rm iso}^{\rm ZPVC}$, the total (electronic + vibrational) isotropic measure of the α tensor. All values are provided in bohr^3.

Method	$\alpha_{\rm iso}^{\rm ZPVC}$	$\alpha_{\rm aniso}^{\rm ZPVC}$	$\alpha_{\rm iso}$	$\alpha_{\rm aniso}$	$\eta_{\rm iso0}$ (%)[a]	$\eta_{\rm aniso}$ (%)[a]	$\alpha_{\rm iso}^{\rm total}$	References
HF	0.247	0.268	8.505	1.148	2.91	23.36	8.752	54
HF	0.180	0.230	8.500	0.910	2.12	25.27	8.680	57
HF	0.130	0.180	7.990	1.380	1.63	13.04	8.120	16
HF	0.249	0.281	8.479	1.181	2.94	23.79	8.728	28
CPHF/TD-HF	0.247	0.268	8.362	...	2.96	...	8.609	58 and 59
MP2	0.292	0.242	9.792	0.426	2.98	56.71	10.084	54
MP2	0.160	0.170	9.250	1.330	1.73	12.78	9.410	16
MP2	0.292	0.242	9.944	0.528	2.94	45.83	10.236	60
CASSCF	0.360	...	9.500	...	3.79	...	9.860	27
CASSCF	0.282	0.272	9.269	0.636	3.04	42.66	9.550	28
CASSCF	0.287	0.270	9.394	0.543	3.06	49.72	9.681	29
CCSD	0.308	0.283	9.632	0.557	3.20	50.81	9.940	37
VSCF[b]	0.285	0.264	9.638	0.537	2.96	49.16	9.923	39
FVCI[b]	0.285	0.265	9.638	0.537	2.96	49.35	9.923	39
PBE	0.270	...	10.590	...	2.55	...	10.860	51
B97-2	0.175	...	9.745	...	1.80	...	9.920	26
BOMD-ωB97X-D	0.220	...	9.650	...	2.28	...	9.870	41
CCSDT[c]	0.292	0.269	9.539	0.565	3.06	47.70	9.831	...

[a] $\eta_{\rm iso} \equiv (\alpha_{\rm iso}^{\rm ZPVC}/\alpha_{\rm iso}) \times 100$. $\eta_{\rm aniso} \equiv (\alpha_{\rm aniso}^{\rm ZPVC}/\alpha_{\rm aniso}) \times 100$.
[b] Electronic contributions were computed at the CCSD/daTZ level.
[c] This work. Electronic contributions were computed at the LR-CCSDT/daQZ+$\Delta\alpha_{\rm basis}$+$\Delta\alpha_{\rm core}$ level.

respectively, which are similar in magnitude to several previously reported studies, including CCSD[37] and VSCF/FVCI.[39] In this work, which represents the highest level of theory used to date for computing $\alpha^{\rm ZPVC}$, we find that the individual ZPVC contributions to $\alpha_{\rm iso}$ ($\alpha_{\rm aniso}$) originating from bending, symmetric stretching, and asymmetric stretching were found as 0.0322 (0.0170), 0.1358 (0.1387), and 0.1236 (0.1162) bohr^3, respectively. As expected from the discussion above, the two stretching modes dominate the vibrational contribution to both $\alpha_{\rm iso}$ and $\alpha_{\rm aniso}$. In this regard, the magnitude of both $\alpha_{\rm iso}^{\rm ZPVC}$ and $\alpha_{\rm aniso}^{\rm ZPVC}$ has a weak dependence on the underlying level of theory, but their contribution to $\alpha_{\rm iso}^{\rm total}$ and $\alpha_{\rm aniso}^{\rm total}$ is far from negligible. For $\alpha_{\rm iso}^{\rm total}$, we find that the vibrational contribution represents ≈3% of the electronic contribution to $\alpha_{\rm iso}$. On the other hand, $\alpha_{\rm aniso}^{\rm ZPVC}$ is comparable in magnitude with the corresponding electronic contribution, representing nearly 50% of $\alpha_{\rm aniso}$ (see Table VIII).

Our static isotropic dipole polarizability including ZPVC for a H_2O molecule in its ground vibrational state, $\alpha_{\rm iso}^{\rm total} = \alpha_{\rm iso} + \alpha_{\rm iso}^{\rm ZPVC} = 9.8307$ bohr^3, essentially reproduces the experimental estimate of 9.83 ± 0.02 bohr^3 derived by Russell and Spackman[54] using a quadratic extrapolation of experimental refractivity data[82] contained within a frequency window of 0.06793–0.09495 a.u. Although the pure vibrational contribution to α may (in general) be important, this term can be ignored for experiments involving UV-Visible radiation (i.e., for frequencies larger than 0.05 a.u.) such as that described above.[124,154,155] We note in passing that there is an alternative extrapolation based on the measurements by Newbound[84] which yields a value of 9.703 ± 0.013 bohr^3.[83] In this regard, the excellent agreement between our benchmark theoretical results and the experimental value by Russell and Spackman provides further validation that the experimental estimate of $\alpha_{\rm iso}^{\rm total} = 9.83 \pm 0.02$ bohr^3 is quite reliable and the error margins might in fact be overestimated.

From the data in Table VIII, it is undoubtedly clear that a high-order electron-correlation method combined with a sufficiently large basis set is essential for obtaining accurate predictions of $\alpha_{\rm iso}^{\rm total}$ and $\alpha_{\rm aniso}^{\rm total}$ for a water molecule. In most cases, one can still obtain satisfactory estimates of these quantities, but this level of accuracy is largely fortuitous, as it is often based on a favorable error cancellation between $\alpha_{\rm iso}$ ($\alpha_{\rm aniso}$) and $\alpha_{\rm iso}^{\rm ZPVC}$ ($\alpha_{\rm aniso}^{\rm ZPVC}$). For example, the second best result from all previous studies in Table VIII (when compared to the experimental estimate of $\alpha_{\rm iso}^{\rm total} = 9.83 \pm 0.02$ bohr^3) was obtained via a Born-Oppenheimer molecular dynamics (BOMD) simulation employing the ωB97X-D functional, which yielded a final value of 9.87 bohr^3 for $\alpha_{\rm iso}^{\rm total}$. Upon closer inspection, however, this otherwise excellent value (which slightly overestimates the experimental estimate by 0.2%–0.6%) is largely based on a cancellation of errors between $\alpha_{\rm iso}$ (which is overestimated by 1.2%) and $\alpha_{\rm iso}^{\rm ZPVC}$ (which is underestimated by 24.7%), when compared to the values of these quantities computed herein. For convenience, we have provided our final recommended values for the electronic and vibrational contributions to the non-zero components of the molecular α (as well as $\alpha_{\rm iso}$ and $\alpha_{\rm aniso}$) for a H_2O molecule in its ground vibrational state in Table IX. All of these contributions were computed

TABLE IX. Summary of the current benchmark values (in bohr^3) provided in this work for the electronic and vibrational contributions to the static dipole polarizability components (α_{xx}, α_{yy}, α_{zz}) of the H_2O molecule in its ground vibrational state, as well as the corresponding isotropic (α_{iso}) and anisotropic (α_{aniso}) measures of this tensor. As described in the main text, the electronic contributions were computed using the experimental geometry (r_0 = 0.9578 Å and θ_0 = 104.4776°) and include a baseline calculation at the LR-CCSDT/daQZ level ($\alpha^{\text{LR-CCSDT/daQZ}}$) as well as further corrections for basis set incompleteness error ($\Delta\alpha_{\text{basis}}$ = LR-CCSD/da5Z–LR-CCSD/daQZ) and core electron contributions ($\Delta\alpha_{\text{core}}$ = LR-CCSD[FULL]/daCQZ–LR-CCSD/daQZ), as given in Eqs. (8)–(10). The vibrational contribution (α^{ZPVC}) was computed with CCSDT/daTZ using the geometry optimized at the same level (r_e = 0.9617 Å and θ_e = 104.1713°). The final recommended values for the electronic and total (electronic + vibrational) contributions to α are given by $\alpha = \alpha^{\text{LR-CCSDT/daQZ}} + \Delta\alpha_{\text{basis}} + \Delta\alpha_{\text{core}}$ and $\alpha^{\text{total}} = \alpha + \alpha^{\text{ZPVC}}$, respectively.

	$\alpha^{\text{LR-CCSDT/daQZ}}$	$\Delta\alpha_{\text{basis}}$	$\Delta\alpha_{\text{core}}$	α	α^{ZPVC}	α^{total}
α_{xx}	9.9282	–0.0227	–0.0311	9.8744	0.4422	10.3166
α_{yy}	9.3114	–0.0357	–0.0524	9.2233	0.1317	9.3550
α_{zz}	9.5829	–0.0260	–0.0374	9.5196	0.3009	9.8205
α_{iso}	9.6075	–0.0281	–0.0403	9.5391	0.2916	9.8307
α_{aniso}	0.5354	0.0117	0.0189	0.5645	0.2693	0.8338

at the (LR-)CCSDT level of theory and represent the most accurate theoretical values available to date.

IV. CONCLUSIONS

In this work, the geometric dependence of the static dipole polarizability of a water molecule was investigated by explicitly computing the corresponding dipole polarizability surface (DPS) across 3125 total (1625 symmetry-unique) geometries using linear response coupled cluster theory including single, double, and triple excitations (LR-CCSDT) and the doubly augmented triple-ζ basis set (d-aug-cc-pVTZ). Such high-level quantum chemical calculations include a simultaneous treatment of both electron correlation and basis set effects and were used to generate the corresponding DPS-H_2O-3K database. Analytical formulae based on a power series expansion of this *ab initio* surface were obtained using linear least-squares analysis and provide highly accurate and computationally tractable estimates of these quantities as a function of molecular geometry.

An additional benchmark database (denoted by DPS-H_2O-25++) was also assembled for 25 select geometries (chosen to span the same space as the more extensive collection of 3125 geometries above) and includes even further corrections for basis set incompleteness error and core electron contributions to this fundamental quantity of interest. The benchmark DPS-H_2O-25++ database was then utilized to assess the importance of these effects as well as the relative accuracy obtained using several quantum chemical methods and a library of density functional approximations. In addition to high-level quantum chemical methods like CCSD and the aforementioned least-squares formulae (3K-FIT), we find that the SCAN0, PBE0, MN15, and B97-2 hybrid functionals yield the most accurate descriptions of the molecular polarizability tensor in H_2O. Benchmark values for the leading-order C_6 dispersion coefficients in this set of 25 molecular geometries were also computed using frequency-dependent polarizabilities obtained via the Cauchy moment expansion at the LR-CCSD level with further corrections for basis set and core electron contributions. This procedure has yielded the so-called C6S-H_2O-25++ benchmark database, which represents the most accurate theoretical values of C_6 for the water molecule obtained to date.

A detailed analysis of the vibrational contributions to the dipole polarizability for a H_2O molecule in its ground vibrational state was also performed using first-order perturbation theory at the CCSDT/d-aug-cc-pVTZ level of theory. In doing so, we found that the magnitude of this correction to the isotropic and anisotropic measures of the dipole polarizability tensor is far from negligible and represents approximately 3% and 50% of the electronic contributions to these quantities, respectively. By including electronic and vibrational contributions in our estimate of the total dipole polarizability—both of which were computed using the highest level of theory to date—we obtain a value of 9.8307 bohr^3, which is in perfect agreement with the experimental value of 9.83 ± 0.02 bohr^3.[54] As such, our nearly exact theoretical results for this quantity provide strong support for the above experimental estimate of Russell and Spackman and should therefore largely settle the debate associated with the range of experimental results for this quantity.[54,82–87]

SUPPLEMENTARY MATERIAL

See supplementary material for the tabulated values, least-squares fits, and heat maps for the DPS-H_2O-3K database.

ACKNOWLEDGMENTS

This work was supported by start-up funds from the College of Arts and Sciences at Cornell University. This research used resources of the National Energy Research Scientific Computing Center, which is supported by the Office of Science of the U.S. Department of Energy under Contract No. DE-AC02-05CH11231.

[1] K. D. Bonin and V. V. Kresin, *Electric-Dipole Polarizabilities of Atoms, Molecules, and Clusters* (World Scientific, Singapore, 1997).
[2] L. Piela, *Ideas of Quantum Chemistry*, 2nd ed. (Elsevier, Amsterdam, Netherlands, 2013).
[3] A. J. Stone, *The Theory of Intermolecular Forces*, 2nd ed. (Oxford University Press, Oxford, UK, 2013).
[4] T. Helgaker *et al.*, Chem. Rev. **112**, 543 (2012).
[5] E. Harder, J. D. Eaves, A. Tokmakoff, and B. J. Berne, Proc. Natl. Acad. Sci. U. S. A. **102**, 11611 (2005).
[6] S. Y. Willow, X. C. Zeng, S. S. Xantheas, K. S. Kim, and S. Hirata, J. Phys. Chem. Lett. **7**, 680 (2016).
[7] V. Babin, C. Leforestier, and F. Paesani, J. Chem. Theory Comput. **9**, 5395 (2013).
[8] J. F. Ouyang and R. P. A. Bettens, CHIMIA Int. J. Chem. **69**, 104 (2015).
[9] Y. Mei *et al.*, J. Phys. Chem. A **119**, 5865 (2015).
[10] H. Jiang, O. A. Moultos, I. G. Economou, and A. Z. Panagiotopoulos, J. Phys. Chem. B **120**, 12358 (2016).
[11] J. R. Hammond, N. Govind, K. Kowalski, J. Autschbach, and S. S. Xantheas, J. Chem. Phys. **131**, 214103 (2009).
[12] M. A. Spackman, J. Phys. Chem. **93**, 7594 (1989).
[13] P. E. S. Wormer and H. Hettema, J. Chem. Phys. **97**, 5592 (1992).
[14] C. Voisin, A. Cartier, and J. L. Rivail, J. Phys. Chem. **96**, 7966 (1992).
[15] F. Aiga and R. Itoh, Chem. Phys. Lett. **251**, 372 (1996).
[16] J. M. Luis, M. Duran, and J. L. Andrés, J. Chem. Phys. **107**, 1501 (1997).
[17] D. Spelsberg and W. Meyer, J. Chem. Phys. **108**, 1532 (1998).

[18]G. Maroulis, Chem. Phys. Lett. **289**, 403 (1998).
[19]D. J. Tozera and N. C. Handy, J. Chem. Phys. **109**, 10180 (1998).
[20]A. J. Cohen and Y. Tantirungrotechai, Chem. Phys. Lett. **299**, 465 (1999).
[21]A. V. Gubskaya and P. G. Kusalik, Mol. Phys. **99**, 1107 (2001).
[22]M. Torrent-Sucarrat, J. M. Luis, and B. Kirtman, J. Chem. Phys. **122**, 204108 (2005).
[23]R. J. Wheatley, J. Comput. Chem. **29**, 445 (2008).
[24]D. M. Elking, L. Perera, R. Duke, T. Darden, and L. G. Pedersen, J. Comput. Chem. **32**, 3283 (2011).
[25]A. J. Thakkar and T. Wu, J. Chem. Phys. **143**, 144302 (2015).
[26]A. S. Sharipov, B. I. Loukhovitski, and A. M. Starik, J. Phys. B: At., Mol. Opt. Phys. **50**, 165101 (2017).
[27]Y. Luo *et al.*, J. Chem. Phys. **98**, 7159 (1993).
[28]K. Ruud, P.-O. Åstrand, and P. R. Taylor, J. Chem. Phys. **112**, 2668 (2000).
[29]K. Ruud, D. Jonssona, and P. R. Taylor, Phys. Chem. Chem. Phys. **2**, 2161 (2000).
[30]J. Páleníková, M. Kraus, P. Neogrády, V. Kellö, and M. Urban, Mol. Phys. **106**, 2333 (2008).
[31]H. Sekino and R. J. Bartlett, J. Chem. Phys. **98**, 3022 (1993).
[32]T. Pluta, J. Noga, and R. J. Bartlett, Int. J. Quantum Chem. **52**, 379 (1994).
[33]B. Datta, P. Sen, and D. Mukherjee, J. Phys. Chem. **99**, 6441 (1995).
[34]A. G. Ioannou, S. M. Colwell, and R. D. Amos, Chem. Phys. Lett. **278**, 278 (1997).
[35]E. K. Dalskov and S. P. A. Sauer, J. Phys. Chem. A **102**, 5269 (1998).
[36]O. Christiansen, J. Gauss, and J. F. Stanton, Chem. Phys. Lett. **305**, 147 (1999).
[37]G. Avila, J. Chem. Phys. **122**, 144310 (2005).
[38]P. Sałek *et al.*, Mol. Phys. **103**, 439 (2005).
[39]J. Kongsted and O. Christiansen, J. Chem. Phys. **125**, 124108 (2006).
[40]T. Korona, Phys. Chem. Chem. Phys. **12**, 14977 (2010).
[41]R. Monten, B. Hajgató, and M. S. Deleuze, Mol. Phys. **109**, 2317 (2011).
[42]A. Heßelmann, Mol. Phys. **111**, 1249 (2013).
[43]A. S. Karne *et al.*, Chem. Phys. Lett. **635**, 168 (2015).
[44]O. Loboda, F. Ingrosso, M. F. Ruiz-López, H. Reis, and C. Millot, J. Comput. Chem. **37**, 2125 (2016).
[45]A. Karton and J. M. L. Martin, J. Chem. Phys. **133**, 144102 (2010).
[46]S. J. A. van Gisbergen *et al.*, J. Chem. Phys. **105**, 3142 (1996).
[47]D. Porezag and M. R. Pederson, Phys. Rev. B **54**, 7830 (1996).
[48]P. Calaminici, K. Jug, and A. M. Köster, J. Chem. Phys. **109**, 7756 (1998).
[49]C. Van Caillie and R. D. Amos, Chem. Phys. Lett. **328**, 446 (2000).
[50]P. J. Wilson, T. J. Bradley, and D. J. Tozer, J. Chem. Phys. **115**, 9233 (2001).
[51]M. R. Pederson, T. Baruah, P. B. Allen, and C. Schmidt, J. Chem. Theory Comput. **1**, 590 (2005).
[52]X. Andrade, S. Botti, M. A. L. Marques, and A. Rubio, J. Chem. Phys. **126**, 184106 (2007).
[53]D. M. Bishop and L. M. Cheung, J. Phys. Chem. Ref. Data **11**, 119 (1982).
[54]A. J. Russell and M. A. Spackman, Mol. Phys. **84**, 1239 (1995).
[55]D. M. Bishop, Rev. Mod. Phys. **62**, 343 (1990).
[56]D. M. Bishop, Adv. Chem. Phys. **104**, 1 (1998).
[57]H.-J. Werner and W. Meyer, Mol. Phys. **31**, 855 (1976).
[58]J. M. Luis, M. Duran, J. L. Andrés, B. Champagne, and B. Kirtman, J. Chem. Phys. **111**, 875 (1999).
[59]O. Quinet, B. Champagne, and B. Kirtman, J. Comput. Chem. **22**, 1920 (2001).
[60]H. Reisa, S. Raptis, and M. Papadopoulos, Chem. Phys. **263**, 301 (2001).
[61]Y. Wang, X. Huang, B. C. Shepler, B. J. Braams, and J. M. Bowman, J. Chem. Phys. **134**, 094509 (2011).
[62]V. Babin, G. R. Medders, and F. Paesani, J. Chem. Theory Comput. **10**, 1599 (2014).
[63]G. R. Medders, V. Babin, and F. Paesani, J. Chem. Theory Comput. **10**, 2906 (2014).
[64]P. Jankowski *et al.*, J. Phys. Chem. A **119**, 2940 (2015).
[65]D. M. Bishop and L. M. Cheung, Chem. Phys. Lett. **66**, 467 (1979).
[66]C. E. Dykstra, J. Chem. Educ. **65**, 198 (1988).
[67]M. Kállay and J. Gauss, J. Mol. Struct.: THEOCHEM **768**, 71 (2006).
[68]K. D. Nanda and A. I. Krylov, J. Chem. Phys. **145**, 204116 (2016).
[69]D. E. Woon and T. H. Dunning, Jr., J. Chem. Phys. **100**, 2975 (1994).
[70]G. R. Medders, A. W. Götz, M. A. Morales, P. Bajaj, and F. Paesani, J. Chem. Phys. **143**, 104102 (2015).
[71]A. Grisafi, D. M. Wilkins, G. Csányi, and M. Ceriotti, Phys. Rev. Lett. **120**, 036002 (2018).
[72]T. Bereau, R. A. DiStasio, Jr., A. Tkatchenko, and O. A. von Lilienfeld, J. Chem. Phys. **148**, 241706 (2018).
[73]H. Partridge and D. W. Schwenke, J. Chem. Phys. **106**, 4618 (1997).
[74]O. L. Polyansky *et al.*, Science **299**, 539 (2003).
[75]A. G. Császár *et al.*, J. Chem. Phys. **122**, 214305 (2005).
[76]G. S. Fanourgakis and S. S. Xantheas, J. Phys. Chem. A **110**, 4100 (2006).
[77]C. J. Burnham and S. S. Xantheas, J. Chem. Phys. **116**, 5115 (2002).
[78]G. S. Fanourgakis and S. S. Xantheas, J. Chem. Phys. **128**, 074506 (2008).
[79]C. J. Burnham, D. J. Anick, P. K. Mankoo, and G. F. Reiter, J. Chem. Phys. **128**, 154519 (2008).
[80]R. Bukowski, K. Szalewicz, G. C. Groenenboom, and A. van der Avoird, Science **315**, 1249 (2007).
[81]Y. Wang and J. M. Bowman, J. Chem. Phys. **134**, 154510 (2011).
[82]C. Cuthbertson and M. Cuthbertson, Philos. Trans. R. Soc. A **213**, 1 (1914).
[83]R. Bukowski, K. Szalewicz, G. C. Groenenboom, and A. van der Avoird, J. Chem. Phys. **128**, 094313 (2008).
[84]K. B. Newbound, J. Opt. Soc. Am. **39**, 835 (1949).
[85]H. Barrell and J. E. Sears, Philos. Trans. R. Soc. A **238**, 1 (1939).
[86]G. D. Zeiss and W. J. Meath, Mol. Phys. **30**, 161 (1975).
[87]U. Hohm, J. Mol. Struct. **1054-1055**, 282 (2013).
[88]A. R. Hoy and P. R. Bunker, J. Mol. Spectrosc. **74**, 1 (1979).
[89]T. Hasegawa and Y. Tanimura, J. Phys. Chem. B **115**, 5545 (2011).
[90]O. Loboda, F. Ingrosso, M. F. Ruiz-López, K. Szalewicz, and C. Millot, J. Chem. Phys. **144**, 034304 (2016).
[91]O. Loboda and C. Millot, J. Chem. Phys. **147**, 161718 (2017).
[92]D. E. Woon and T. H. Dunning, Jr., J. Chem. Phys. **103**, 4572 (1995).
[93]P. A. M. Dirac, Math. Proc. Cambridge Philos. Soc. **26**, 376 (1930).
[94]S. H. Vosko, L. Wilk, and M. Nusair, Can. J. Phys. **58**, 1200 (1980).
[95]A. D. Becke, Phys. Rev. A **38**, 3098 (1988).
[96]C. Lee, W. Yang, and R. G. Parr, Phys. Rev. B **37**, 785 (1988).
[97]J. P. Perdew, K. Burke, and M. Ernzerhof, Phys. Rev. Lett. **77**, 3865 (1996).
[98]A. D. Becke, J. Chem. Phys. **98**, 5648 (1993).
[99]P. J. Stephens, F. J. Devlin, C. F. Chabalowski, and M. J. Frisch, J. Phys. Chem. **98**, 11623 (1994).
[100]C. Adamo and V. Barone, J. Chem. Phys. **110**, 6158 (1999).
[101]R. Peverati and D. G. Truhlar, J. Phys. Chem. Lett. **2**, 2810 (2011).
[102]J.-D. Chai and M. Head-Gordon, Phys. Chem. Chem. Phys. **10**, 6615 (2008).
[103]H. S. Yu, X. He, S. L. Li, and D. G. Truhlar, Chem. Sci. **7**, 5032 (2016).
[104]N. Mardirossian and M. Head-Gordon, J. Chem. Phys. **142**, 074111 (2015).
[105]N. Mardirossian and M. Head-Gordon, Phys. Chem. Chem. Phys. **16**, 9904 (2014).
[106]N. Mardirossian and M. Head-Gordon, J. Chem. Phys. **144**, 214110 (2016).
[107]J. Sun *et al.*, J. Chem. Phys. **138**, 044113 (2013).
[108]J. Sun, J. P. Perdew, and A. Ruzsinszky, Proc. Natl. Acad. Sci. U. S. A. **112**, 685 (2015).
[109]J. Sun, A. Ruzsinszky, and J. Perdew, Phys. Rev. Lett. **115**, 036402 (2015).
[110]K. Hui and J.-D. Chai, J. Chem. Phys. **144**, 044114 (2016).
[111]J. Wellendorff, K. T. Lundgaard, K. W. Jacobsen, and T. Bligaard, J. Chem. Phys. **140**, 144107 (2014).
[112]H. B. G. Casimir and B. Polder, Phys. Rev. **73**, 360 (1948).
[113]C. Hättig, O. Christiansen, and P. Jørgensen, J. Chem. Phys. **107**, 10592 (1997).
[114]O. Christiansen, A. Halkier, H. Koch, and P. Jørgensen, J. Chem. Phys. **108**, 2801 (1998).
[115]P. W. Langhoff and M. Karplus, J. Chem. Phys. **53**, 233 (1970).
[116]O. Christiansen, H. Koch, and P. Jørgensen, Chem. Phys. Lett. **243**, 409 (1995).
[117]G. Chałasiński and M. M. Szczęśniak, Mol. Phys. **63**, 205 (1988).
[118]S. M. Cybulski, G. Chałasiński, and R. Moszyński, J. Chem. Phys. **92**, 4357 (1990).
[119]S. M. Cybulski and M. L. Lytle, J. Chem. Phys. **127**, 141102 (2007).
[120]A. Tkatchenko, R. A. DiStasio, Jr., M. Head-Gordon, and M. Scheffler, J. Chem. Phys. **131**, 094106 (2009).
[121]W. Rijks and P. E. S. Wormer, J. Chem. Phys. **88**, 5704 (1988).
[122]A. Osted, J. Kongsted, K. V. Mikkelsen, and O. Christiansen, J. Phys. Chem. A **108**, 8646 (2004).
[123]J. Marti and D. M. Bishop, J. Chem. Phys. **99**, 3860 (1993).
[124]D. M. Bishop and S. P. A. Sauer, J. Chem. Phys. **107**, 8502 (1997).
[125]A. R. Hoy, I. M. Mills, and G. Strey, Mol. Phys. **24**, 1265 (1972).
[126]H. H. Nielsen, Rev. Mod. Phys. **23**, 90 (1951).
[127]P. W. Fowler, Mol. Phys. **43**, 591 (1981).
[128]P. W. Fowler, Mol. Phys. **51**, 1423 (1984).
[129]W. Schneider and W. Thiel, Chem. Phys. Lett. **157**, 367 (1989).
[130]J. R. Hammond, K. Kowalski, and W. A. deJong, J. Chem. Phys. **127**, 144105 (2007).

[131] J. R. Hammond, M. Valiev, W. A. deJong, and K. Kowalski, J. Phys. Chem. A **111**, 5492 (2007).
[132] J. R. Hammond, W. A. deJong, and K. Kowalski, J. Chem. Phys. **128**, 224102 (2008).
[133] M. Valiev *et al.*, Comput. Phys. Comm. **181**, 1477 (2010).
[134] K. Aidas *et al.*, Wiley Interdiscip. Rev.: Comput. Mol. Sci. **4**, 269 (2014).
[135] DALTON, a molecular electronic structure program, Release Dalton2016.0, 2015, see http://daltonprogram.org.
[136] Y. Shao *et al.*, Mol. Phys. **113**, 184 (2015).
[137] P. M. W. Gill, B. G. Johnson, and J. A. Pople, Chem. Phys. Lett. **209**, 506 (1993).
[138] O. A. Vydrov and T. Van Voorhis, J. Chem. Phys. **133**, 244103 (2010).
[139] The range of $\alpha_{xz} \approx 0$–4 bohr^3 applies to water molecules with $r_1 \leq r_2$ (for water molecules with $r_1 > r_2$, there will be a sign change in this component).
[140] T. Brinck, J. S. Murray, and P. Politzer, J. Chem. Phys. **98**, 4305 (1993).
[141] M. Thomas, M. Brehm, R. Fligg, P. Vöhringer, and B. Kirchner, Phys. Chem. Chem. Phys. **15**, 6608 (2013).
[142] W. Kabsch, Acta Cryst. A **32**, 922 (1976).
[143] T. Janowski and P. Pulay, Chem. Phys. Lett. **447**, 27 (2007).
[144] S. K. Min *et al.*, J. Comput. Chem. **29**, 1208 (2008).
[145] C. D. Sherrill, T. Takatani, and E. G. Hohenstein, J. Phys. Chem. A **113**, 010146 (2009).
[146] M. S. Marshall, L. A. Burns, and C. D. Sherrill, J. Chem. Phys. **135**, 194102 (2011).
[147] G. D. Zeiss and W. J. Meath, Mol. Phys. **33**, 1155 (1977).
[148] K. U. Lao and J. M. Herbert, J. Phys. Chem. A **119**, 235 (2015).
[149] K. U. Lao, R. Schäffer, G. Jansen, and J. M. Herbert, J. Chem. Theory Comput. **11**, 2473 (2015).
[150] K. U. Lao, K.-Y. Liu, R. M. Richard, and J. M. Herbert, J. Chem. Phys. **144**, 164105 (2016).
[151] D. Hait and M. Head-Gordon, Phys. Chem. Chem. Phys. **20**, 19800 (2018).
[152] T. Korona, M. Przybytek, and B. Jeziorski, Mol. Phys. **104**, 2303 (2006).
[153] R. D. Amos, Adv. Chem. Phys. **67**, 99 (1987).
[154] O. Christiansen, C. Hättig, and J. Gauss, J. Chem. Phys. **109**, 4745 (1998).
[155] F. Egidi *et al.*, J. Chem. Theory Comput. **10**, 2456 (2014).
[156] E. Bichoutskaia, M. P. Hodges, and R. J. Wheatley, J. Comput. Methods Sci. Eng. **2**, 391 (2002).
[157] A. S. Tulegenov, R. J. Wheatley, M. P. Hodges, and A. H. Harvey, J. Chem. Phys. **126**, 094305 (2007).